ELSEVIER

Chemistry and Physics of Lipids
100 (1999) 3–31

CPL
CHEMISTRY AND PHYSICS OF LIPIDS

www.elsevier.com/locate/chemphyslip

# Inhibition of human gastric and pancreatic lipases by chiral alkylphosphonates. A kinetic study with 1,2-didecanoyl-*sn*-glycerol monolayer

Jean-François Cavalier [a], Stéphane Ransac [b], Robert Verger [b], Gérard Buono [a,*]

[a] *ENSSPICAM, UMR 6516, "Synthèse, Catalyse et Chiralité", avenue Escadrille Normandie-Niemen, F-13397 Marseille, Cedex 20, France*

[b] *Laboratoire de Lipolyse Enzymatique, UPR 9025, IFR 1 du CNRS, 31, Chemin Joseph Aiguier, F-13402 Marseille, Cedex 20, France*

Received 20 July 1998; received in revised form 18 January 1999; accepted 21 January 1999

**Abstract**

Enantiomerically pure alkylphosphonate compounds RR′P(O)PNP ($R = C_nH_{2n+1}$, $R' = OY$ with $Y = C_{n'}H_{2n'+1}$ with $n = n'$ or $n \neq n'$; PNP = *p*-nitrophenoxy) noted (RY), mimicking the transition state occurring during the carboxyester hydrolysis were synthesized and investigated as potential inhibitors of human gastric lipase (HGL) and human pancreatic lipase (HPL). The inhibitory properties of each enantiomer have been tested with the monomolecular films technique in addition to an enyzme linked immunosorbent assay (ELISA) in order to estimate simultaneously the residual enzymatic activity as well as the interfacial lipase binding. With both lipases, no obvious correlation between the inhibitor molar fraction ($\alpha_{50}$) leading to half inhibition, and the chain length, R or Y was observed. ($R_{11}Y_{16}$)s were the best inhibitor of HPL and ($R_{10}Y_{11}$)s were the best inhibitors of HGL. We observed a highly enantioselective discrimination, both with the pure enantiomeric alkylphosphonate inhibitors as well as a scalemic mixture. We also showed, for the first time, that this enantioselective recognition can occur either during the catalytic step or during the initial interfacial adsorption step of the lipases. These experimental results were analyzed with two kinetic models of covalent as well as pseudo-competitive inhibition of lipolytic enzymes by two enantiomeric inhibitors. 

*Keywords:* Lipase enantioselective recognition; Chiral alkylphosphonates; Human gastric and pancreatic lipases; Monomolecular film technique

* Corresponding author. Fax: +33-491-027776.
*E-mail addresses:* verger@ir2cbm.cnrs-mrs.fr (R. Verger), buono@spi-chim.u-3mrs.fr (G. Buono)

0009-3084/99/$ - see front matter 
PII: S0009-3084(99)00028-6

## 1. Introduction

Lipases have potential applications in chemistry (Rogalska et al., 1997; Schmid and Verger, 1998), biotechnology (Vulfson, 1994; Ransac et al., 1996) and medicine. In the latter domain, for instance, conventional weight-reducing strategies have focused largely on controlling the energy intake, but there is a doubt as to the long-term efficacy of these approaches. Reducing the adsorption of dietary fat by prescribing digestive lipases inhibitors holds great promise as an anti-obesity strategy (Güzelhan et al., 1991; Drent and Vanderveen, 1993; Güzelhan et al., 1994; Drent and Vanderveen, 1995; Drent et al., 1995). Furthermore, designing and synthesizing specific inhibitors is of fundamental value for understanding the molecular mechanisms involved in the interfacial adsorption step as well as the catalytic activity of lipases.

Among the range of esterase inhibitors, phosphonate compounds present a fundamental interest to understand the mechanisms of catalysis. These compounds RR′P(O)PNP, noted (RY), mimicking in both their charge distribution and geometry the first transition states occurring during carboxyester hydrolysis were synthesized and investigated as potential inhibitors of human gastric (HGL) and pancreatic (HPL) lipases (Marguet et al., 1994; Gargouri et al., 1997). Their efficiency was studied on the basis of the alkyl chain length, the nature of the leaving group and the influence of the ester substituent (Marguet et al., 1994). The released *p*-nitrophenol to enzyme ratio indicates the formation of a 1:1 complex. In the absence of substrate, the most powerful inhibitor was *O*-methyl-*O*-(*p*-nitrophenyl) *n*-pentylphosphonate, ($R_5Y_1$), which possessed a short alkyl chain ($R = C_5H_{11}$), a small methoxy ester substituent ($Y = CH_3$) and a good leaving group.

Enantioselective inhibition was described for the first time by Patkar and Björkling using *Candida antartica* and *Rhizomucor miehei* lipases with pure enantiomers of *O*-ethyl-*O*-(*p*-nitrophenyl) *n*-hexylphosphonate ($R_6Y_2$) as inhibitors (Björkling et al., 1994; Patkar and Björkling, 1994). Furthermore, using both diastereomers ($S_p$, $R_p$)-1*R*-Cl or ($S_p$, $R_p$)-1*S*-Cl of *O*-menthyl *n*-hexyl chlorophosphonate as inhibitors of *Candida rugosa* lipase, Cygler et al. have provided a structural basis of the chiral preferences of lipases (Cygler et al., 1994). It is worth noting that both phosphonate groups were covalently bound to the Oγ oxygen of the serine 209, and presented a ($S_p$) stereochemistry, assuming that only the ($S_p$)-1*R*-Cl and ($S_p$)-1*S*-Cl diastereomers in the original mixture of ($S_p$, $R_p$) diastereomers reacted.

Acylglycerol analogues, in which one carbonyl of the hydrolysable ester bonds was replaced by a phosphonate group including a good leaving group, were synthesized as lipase inhibitors (Mannesse et al., 1995; Stadler et al., 1996). In all the cases, the lipases used exhibited a great stereoselectivity towards the chirality of these compounds at the phosphorus and/or the glycerol sites. With respect to HPL and HGL, Marguet et al. studied their inhibition by the monomolecular films technique coupled with ELISA tests, using mixed films of chiral pure *sn*-1,2- and *sn*-2,3-*O*-didecanoylglycerophosphonates and 1,2-dicaprin (Egloff et al., 1995b). With HPL, the four stereoisomers exhibited a rather weak inhibitory power and no significant differences were observed among them. With HGL, however, the inhibition depended much more strongly on the chirality at the *sn*-2 carbon of the glycerol backbone, while the chirality at the phosphorus atom had no influence. Moreover, a clear correlation was observed between the HGL surface concentration and the inhibitor molar fraction ($\alpha_{50}$) leading to half inhibition, the greatest enzymatic inhibition was observed with films containing the enantiomeric inhibitor to which the HGL was best adsorbed (Egloff et al., 1995b). Recently, the three dimensional structure of HPL-colipase complexes covalently bound to each enantiomer of a chiral phosphonate inhibitor, the *O*-methyl-*O*-(*p*-nitrophenyl) *n*-undecylphosphonate ($R_{11}Y_1$), was resolved by X-ray diffraction (Egloff et al., 1995a). The crystal structure of a racemic mixture of ($R_{11}Y_1$) showed that the phosphorus atom of each enantiomer were covalently bound to the $O_\gamma$ oxygen of the active serine 152. Furthermore, the use of each enantiomer separately in the crystallization medium, revealed that the absolute configuration of the phosphorus atom of the most

reactive enantiomer, bound to the catalytic serine, was ($R_p$). The C11 alkyl chain of this first enantiomer fitted into a hydrophobic groove, mimicking the interactions with the leaving acyl chain of a glycerol substrate. The alkyl chain of the second enantiomer (the less reactive bound to the catalytic serine, ($S_p$) configuration) possessed an elongated conformation and interacted with hydrophobic patches on the surface of the open conformation of the amphipathic lid. This was suggestive of the location of a second acyl chain of a glycerol substrate. Finally, the alkyl chains of the two enantiomers superimposed well with the two fatty acyl chains of the phospholipid observed in the ternary phosphatidylcholine-HPL-colipase complex (van Tilbeurgh et al., 1993).

On the basis of these crystallographic studies, and in an attempt to further characterize the catalytic mechanism and in order to improve the molecular fit in the two hydrophobic clefts of the HPL active site, we designed and synthesized new chiral phosphonate inhibitors (RY). Their efficacy was studied by varying successively the alkyl or ester chain length, R and Y respectively, from one to 16 carbon atoms with *p*-nitrophenoxy as leaving group (Scheme 1). In the present paper, we wish to report the synthesis of these alkylphosphonate compounds, and the results of their inhibition studies on HPL and HGL at the air–water interface using the monomolecular films technique coupled with ELISA tests.

## 2. Materials and methods

### 2.1. Materials

1,2-Didecanoyl-*sn*-glycerol (1,2-dicaprin) was purchased from Serdary Research Laboratory (Ont., Canada); streptavidin peroxydase and *O*-phenilenediamine dihydrochloride were purchased from Sigma.

### 2.2. Lipases

HGL and HPL were purified at the laboratory using previously described procedures (De Caro et al., 1977; Moreau et al., 1992). Monoclonal and polyclonal antibodies against either native HGL or native HPL were prepared and characterized as previously described (Ivanova et al., 1993; Aoubala et al., 1993, 1994).

### 2.3. General methods of synthesis

All reactions were carried out under scrupulously dry conditions. All solvents and reagents were purified according to usual methods (Perrin et al., 1980). For TLC, precoated aluminium sheets Merck silica gel 60 $F_{254}$ were employed, and the following detection methods were used: UV lamp (254 nm); PMA, dipped into a solution containing 5% phosphomolibdic acid in absolute ethanol, and heated on a hot plate. All silica chromatographic columns were performed as described by Still et al. (1978) using Merck silica gel 60. Separation of the different enantiomers was performed on a Water HPLC system using a Daicel Chiralpack AS column 250 × 250 mm, and a Waters UV detector at $\lambda = 234$ nm. The HPLC analysis were carried out at 25°C using *n*-hexane–

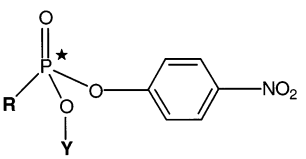


| | | | |
|---|---|---|---|
| $\mathbf{R_{11}}$ = | $C_{11}H_{23}$ | $\mathbf{Y_{11}}$ = | $C_{11}H_{23}$ |
| $\mathbf{Y_1}$ = | $CH_3$ | $\mathbf{R_1}$ = | $CH_3$ |
| $\mathbf{Y_4}$ = | $C_4H_9$ | $\mathbf{R_4}$ = | $C_4H_9$ |
| $\mathbf{Y_6}$ = | $C_6H_{13}$ | $\mathbf{R_6}$ = | $C_6H_{13}$ |
| $\mathbf{Y_8}$ = | $C_8H_{17}$ | $\mathbf{R_8}$ = | $C_8H_{17}$ |
| $\mathbf{Y_{10}}$ = | $C_{10}H_{21}$ | $\mathbf{R_{10}}$ = | $C_{10}H_{21}$ |
| $\mathbf{Y_{12}}$ = | $C_{12}H_{25}$ | $\mathbf{R_{12}}$ = | $C_{12}H_{25}$ |
| $\mathbf{Y_{14}}$ = | $C_{14}H_{29}$ | $\mathbf{R_{14}}$ = | $C_{14}H_{29}$ |
| $\mathbf{Y_{16}}$ = | $C_{16}H_{33}$ | $\mathbf{R_{16}}$ = | $C_{16}H_{33}$ |

Scheme 1. Structure of alkylphosphonates (RY).

2-propanol as eluent; flow rate 4.5 ml $min^{-1}$ (see supplementary material for details). $^{31}P$ NMR experiments were all carried out with a Brucker AC100 FT NMR spectrometer using an 85% $H_3PO_4$ external reference. $^{1}H$ and $^{13}C$ NMR experiments were all carried out with a Brucker AC100 or AC200 FT NMR spectrometer. $CDCl_3$ was used as solvent and internal reference. Rotatory powers were all carried out with a Perkin–Elmer P341 polarimeter. Elemental analyses were performed at the Service Commun de Microanalyse, University of Aix, Marseille III. All products were fully characterised by $^{31}P$, $^{1}H$, $^{13}C$ NMR, elemental analyses and $[\alpha]_D^{20}$.

### 2.4. Synthesis of organophosphorus compounds

#### 2.4.1. Typical experimental procedure for the synthesis of alkylphosphonic acid dichloride 2-$R_{4-16}$ from O-,O-dimethyl alkylphosphonates 1-$R_{4-16}$, described for compound 2-$R_4$

5.2 g (31 mmol) of 1-$R_4$ was added dropwise to a mixture of 11.9 g (87 mol, 3 eq.) of freshly distilled oxalyl chloride in ether (5 ml), and then refluxed for 5 days. After cooling the solution, the excess of reagent was freed in vacuum and the crude product was distilled in vacuum to yield 2-$R_4$ (4.75 g, 79%). $Eb_{0.023} = 50°C$. NMR $^{31}P$: $\delta$ 50.22; $^{1}H$: $\delta$ 2.55 (m, 2H), 1.65 (m, 4H), 0.9 (s, 3H); $^{13}C$: $\delta$ 42.21 (d,P–$CH_2$, $^{1}J_{PC} = 96.4$ Hz), 24.44 (d, P–$CH_2$–$CH_2$, $^{2}J_{PC} = 6.7$ Hz), 22.30 (d, P–$CH_2$–$CH_2$–$CH_2$, $^{3}J_{PC} = 22.2$ Hz), 12.96 ($CH_3$).

#### 2.4.2. Synthesis of methylphosphonic acid dichloride 2-$R_1$

5 g (40 mmol) of 1-$R_1$ was added dropwise to a solution of 10 ml (2.5 eq.) of HCl 33%, and then refluxed for 3 h. The water and methanol formed were then distilled during the reaction. The product was dried under vacuum and $P_2O_5$. 3.84 g (40 mmol, 96%) of methylphosphonic acid thus prepared, were treated by 16.66 g (80 mol, 2 eq.) of phosphorus pentachloride at reflux for 14 h. Phosphorus trichloride was first removed by fractional distillation. Next the crude product was distilled in a vacuum to yield 2-$R_1$ (4.3 g, 81%) as white solid. $Eb_{0.008} = 40°C$; $M_p = 32°C$. $^{31}P$ NMR: $\delta$ 42.9; $^{1}H$ NMR: $\delta$ 2.55 (d, 3H, $J_{PH} = 16{,}3$ Hz); $^{13}C$ NMR: $\delta$ 29.98 (d, P–$CH_3$, $^{1}J_{PC} = 104{,}9$ Hz).

#### 2.4.3. Typical experimental procedure for the preparation of O-alkyl O-(p-nitrophenyl) n-undecylphosphonates ($R_{11}Y_{1-16}$) from 2-$R_{11}$, described for compound ($R_{11}Y_4$)

Under nitrogen, to a solution of 1.0 g (3.66 mmol) *n*-undecylphosphonic acid dichloride 2-$R_{11}$ in $CH_2Cl_2$ (5 ml) freed of ethanol, a solution of 271.5 mg (3.66 mmol) of *n*-butanol 3-$Y_4$, 300.5 mg (3.66 mmol, 1 eq.) of *N*-methylimidazole (NMI) in $CH_2Cl_2$ (5 ml) freed of ethanol was added slowly dropwise. After the first addition, a solution of 509.2 mg (3.66 mmol) of *p*-nitrophenol, 300.5 mg (3.66 mmol, 1 eq.) of NMI in $CH_2Cl_2$ (5 ml) freed of ethanol was then added slowly dropwise. 15 min later, the solvent was removed in vacuum, ether (10 ml) was added and the salts were filtered. The solution was washed seven times with 5% $K_2CO_3$ ($7 \times 5$ ml), once with saturated $NH_4Cl$ (3 ml) and twice with brine. The organic layer was dried ($MgSO_4$), filtered and concentrated in vacuum. The crude product was purified on silica with petroleum ether–ether 7:3 as eluent ($R_f = 0.23$, PMA) to yield ($R_{11}Y_4$) (681 mg, 45%).

HPLC: eluent *n*-hexane–2-propanol 98:2, $t_{R1}$ 14.04 min., $[\alpha]_D^{20} = +2.37$ (*c* 3.63, $CH_2Cl_2$); $t_{R2}$ 15.52 min., $[\alpha]_D^{20} = -2.37$ (*c* 3.63, $CH_2Cl_2$). $^{31}P$ NMR: $\delta$ 29.64; $^{1}H$ NMR: $\delta$ 8.2 (d, $2H_{ar}$, $^{3}J =$ 9.4 Hz), 7.4 (d, $2H_{ar}$, $^{3}J = 10.4$ Hz), 4.2 (m, 2H), 1,9 (m, 2H), 1.7 (m, 2H), 1.3 (m, 20H), 0.9 (t, 6H); $^{13}C$ NMR: $\delta$ 155.72 (d, O–$C_{ar}$, $^{2}J_{PC} = 7.7$ Hz), 144.39 ($C_{ar}$–$NO_2$), 125.52 (O–$C_{ar}$–$C_{ar}$–$C_{ar}$), 120.86 (d, O–$C_{ar}$–$C_{ar}$, $^{3}J_{PC} = 4.8$ Hz), 66.49 (d, O–$CH_2$, $^{2}J_{PC} = 7.24$ Hz), 32.31 (d, O–$CH_2$–$CH_2$, $^{3}J_{PC} = 5.9$ Hz), 31.79 (P–$(CH_2)_8$–$CH_2$), 30.31 (d, P–$CH_2$–$CH_2$–$CH_2$, $^{3}J_{PC} = 16.45$ Hz), 29.22–29.46 (P–$(CH_2)_4$–$(CH_2)_4$), 28.91 (P–$(CH_2)_3$–$CH_2$), 25.81 (d, P–$CH_2$, $^{1}J_{PC} = 139.6$ Hz), 22.58 (P–$(CH_2)_9$–$CH_2$), 22.12 (d, P–$CH_2$–$CH_2$, $^{2}J_{PC} = 5.7$ Hz), 18.57 (O–$CH_2$–$CH_2$–$CH_2$), 13.97 (P–$(CH_2)_{10}$–$CH_3$); 13.39 (O–$(CH_2)_3$–$CH_3$); Anal. Calc. for $C_{21}H_{36}NO_5P$ (413.49): C 61.0, H 8.8, N 3.4, P 7.5%; found, C 62.1, H 8.5, N 3.8, P 7.9%.

*2.4.4. Typical experimental procedure for the preparation of O-(n-undecyl) O-(p-nitrophenyl) alkylphosphonates ($R_{1-16}Y_{11}$) from 2-$R_{1-16}$, described for compound ($R_1Y_{11}$)*

Under nitrogen, to a solution of 1.09 g (8.2 mmol) methylphosphonic acid dichloride 2-$R_1$ in $CH_2Cl_2$ (5 ml) freed of ethanol, a solution of 1.41 mg (8.2 mmol) of *n*-undecanol 3-$Y_{11}$, 674 mg (8.2 mmol, 1 eq.) of NMI in $CH_2Cl_2$ (5 ml) freed of ethanol was added slowly dropwise. After the first addition, a solution of 1.14 mg (8.2 mmol) of *p*-nitrophenol, 674 mg (8.2 mmol, 1 eq.) of NMI in $CH_2Cl_2$ (5 ml) freed of ethanol was then added slowly dropwise. 15 min later, the solvent was removed in vacuum, ether (10 ml) was added and the salts were filtered. The solution was washed seven times with 5% $K_2CO_3$ (7 × 5 ml), once with saturated $NH_4Cl$ (3 ml) and twice with brine. The organic layer was dried ($MgSO_4$), filtered and concentrated in vacuum. The crude product was purified on silica with petroleum ether–ether 1:1 as eluent ($R_f = 0.20$, PMA) to yield ($R_1Y_{11}$) (1.83 g, 60%).

HPLC: eluent *n*-hexane–2-propanol 99.5:0.5, the two enantiomers were not separated. $^{31}$P NMR: $\delta$ 27.40; $^1$H NMR: $\delta$ 8.2 (d, $2H_{ar}$, $^3J = 9.2$ Hz), 7.4 (d, $2H_{ar}$, $^3J = 9.2$Hz), 4.1 (m, 2H), 1.6 (d, 3H, $^1J = 17.65$ Hz), 1.3 (m, 18H), 0.9 (t, 3H); $^{13}$C NMR: $\delta$ 155.49 (d, O–$C_{ar}$, $^2J_{PC} = 8.7$ Hz), 144.69 ($C_{ar}$–$NO_2$), 125.65 (O–$C_{ar}$–$C_{ar}$–$C_{ar}$), 120.91 (d, O–$C_{ar}$–$C_{ar}$, $^3J_{PC} = 4.6$ Hz), 67.05 (d, O–$CH_2$, $^2J_{PC} = 7.2$ Hz), 31.84 (d, O–$(CH_2)_8$–$CH_2$), 30.32 (d, O–$CH_2$–$CH_2$, $^3J_{PC} = 6.8$ Hz), 29.03–29.64 (O–$(CH_2)_3$–$(CH_2)_5$), 25.36 (O–$CH_2$–$CH_2$–$CH_2$), 22.63 (O–$(CH_2)_9$–$CH_2$), 14.05 (O–$(CH_2)_{10}$–$CH_3$), 11.53 (d, P–$CH_3$, $^1J_{PC} = 145.5$ Hz); Anal. calc. for $C_{18}H_{30}NO_5P$ (371.41): C 58.2, H 8.1, N 3.8, P 8.3%; found, C 59.1, H 8.7, N 4.3, P 7.9%.

## 2.5. Monomolecular film experiments

Before each utilization, the Teflon trough was cleaned with tap water, then gently brushed in the presence of distilled ethanol, before being washed again with tap water and finally rinsed with double-distilled water. The aqueous subphase was composed of 10 mM Tris–HCl, pH 8, 100 mM NaCl, 21 mM $CaCl_2$ and 1 mM EDTA for HPL assays or 10 mM sodium acetate–HCl, pH 5, 100 mM NaCl, 21 mM $CaCl_2$ and 1 mM EDTA for HGL assays. Buffers were prepared with double-distilled water and filtered through a 0.45 μM Millipore membrane. Residual surface-active impurities were removed before each assay by sweeping and suction of the surface (Verger and de Haas, 1973).

## 2.6. Enzymes kinetics experiments

Measurements were performed with the KSV 2200 Barostat equipment (KSV-Helsinki). The principle of the method has been described previously by Verger et al. (Verger and de Haas, 1973). It involved the use of a 'zero-order through' with two compartments: a reaction compartment and a reservoir compartment, which were connected to each other by a small surface channel. Enzyme solution was injected into the subphase of the reaction compartment only, whereas the lipid film covered both of them. A mobile barrier, automatically driven by the barostat, moved back and forth over the reservoir to keep the surface pressure ($\pi$) constant, thus compensating for the substrate molecules removed from the film by the enzyme hydrolysis. The surface pressure was measured on the reservoir compartment with a Wilhelmy plate (perimeter 3.94 cm) attached to an electromicrobalance, connected in turn to a microprocessor programmed to regulate the mobile-barrier movement. The reaction compartment was stirred at 250 rpm by two 2.5 cm magnetic bars. The surface of the reaction compartment was 100 cm$^2$ and its volume 100 ml. The reservoir compartment was 148 mm wide and 249 long. Mixed films of substrate–inhibitor were spread from a chloroform solution (about 1 mg ml$^{-1}$), over the surface of the reaction compartment only, whereas the reservoir was covered with a film of pure substrate (1,2-dicaprin) (Piéroni and Verger, 1979, 1983; Gargouri et al., 1987). The kinetics of hydrolysis were recorded for 20–25 mins, and the kinetics data were analyzed as in the case of a previous model (Ransac et al., 1990, 1991).

## 2.7. ELISA tests

The kinetics of hydrolysis were recorded as

described above for 15 min, and the remaining film was aspirated as previously described (Aoubala et al., 1995). The film was recovered into a glass tube (0.3–1 ml) by placing a barrier across the surface channel and by sweeping it over the reaction compartment and aspiring the film thus collected. After completely recovering the film, an equal volume of the sub-phase was sampled and placed in another tube. The difference between the total amounts of proteins between these two samples was attributed to the surface excess of protein molecules bound to the lipid film.

All the ELISA tests were performed in 96-wells poly(vinylchloride) (PVC) microplates (Maxisorb, Nunc). The wells were coated with 250 ng of a specific polyclonal antibody (anti-HGL or anti-HPL for the titration of HGL and HPL respectively) solubilized in 50 μl of 10 mM phosphate buffer (pH 7.5) containing 137 mM NaCl, 2.7 mM KCl and 8 mM $Na_2HPO_4$, 12 $H_2O$ (buffer A) and incubated overnight at 4°C. The wells were then washed three times, 5 min for each, with 300 μl/well of buffer A, and the excess protein binding sites were saturated by incubation with 200 μl/well of blocking agent (3% w/v Régilait skimmed milk powders in buffer A) for 2 h at 37°C. The plates were then washed three times with buffer B (buffer A containing 0.05% v/v Tween 20), and dry the excess buffer by aspiration. Fill each well with 50 μl of sample solution in diluted buffer A, and incubate 1 h at 37°C. Wash the plates three times for 5 min with buffer B, and fill each well with 50 μl of specific biotinylated monoclonal anti-HGL or anti-HPL (detector antibody) in buffer B, and keep at 37°C for 1 h. Wash three times for 5 min with buffer B, and fill each well with 50 μl of Streptavidine peroxydase diluted with buffer B at 1/1000. Keep at 37°C for 45 min. After washing the plates three times for 5 min with buffer B, and drying the excess buffer by aspiration, 50 μl of peroxydase substrate solution (*O*-phenylenediamine dihydrochloride 0.4 g $l^{-1}$ in 100 mM sodium phosphate–150 mM sodium citrate (pH 5) containing 0.04% of fresh hydrogen peroxide) was added to each well and incubated for 15 min in the dark at room temperature. The enzyme reaction was stopped by adding 50 μl of 0.5 M $H_2SO_4$ to each well. The optical density (OD) was measured at 490 nm using a micro ELISA reader (MR 5000, Dynatech).

### 2.8. Determination of the amount of protein adsorbed to the lipid monolayer

A reference curve was drawn up for each test and was used to determine the amount of protein adsorbed to the lipid monolayer. For this purpose, proteins (HGL or HPL) at known concentrations in 50 μl of buffer B were incubated in the wells of a micro-titration plate previously coated with a specific polyclonal antibody. An ELISA was performed as described above. The optical density values at 490 nm were plotted as a function of the concentration of protein. Each assay was carried out in duplicate. The obtained reference curve was used to calculate the concentration of protein in the aspirated samples recovered from the monomolecular experiments as described above. In order to calculate the amount of protein bound to the monomolecular lipid film, the volume occupied by the lipid film was not taken into account since it was negligible with respect to the aspirated sub-phase. We used the following equation:

$$\Gamma = \frac{[F + B] - [B]}{S} \cdot V_a$$

where $\Gamma$ is the surface excess of protein bound to the lipid monolayer, expressed in pg $cm^{-2}$. [F + B] is the concentration of protein present in the aspirated film with the aspirated bulk sub-phase, as determined by ELISA test. [B] is the concentration of protein in the bulk sample, also determined by ELISA. $V_a$ is the aspirated volume (ranging from 0.5 to 1 ml), and $S$ is the area of the reactional compartment of the trough (31 $cm^2$).

### 2.9. Reliability of the sandwich ELISA for HGL and HPL adsorbed lipid monolayers

During the monolayers experiments, the validity of the sandwich ELISA for HGL and HPL was tested in the presence of mixed films of inhibitor–1,2-dicaprin. The recovery levels of protein injected under lipid monomolecular films were determined after each experiment as:

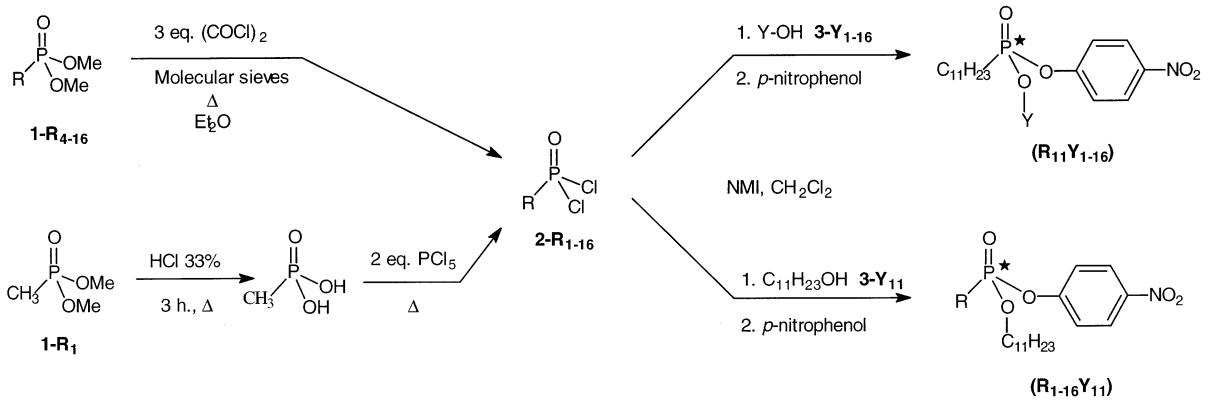


Scheme 2. Synthetic pathway of various alkylphosphonate compounds (RY).

$$\text{Total recovery } (\%) = \frac{[B] \cdot V_t + \Gamma \cdot S}{T} \cdot 100$$

Where [B] is the concentration of HGL or HPL in the sub-phase; $V_t$ is the total volume of the reactional compartment measured after each monolayer experiment ($50 \pm 1.5$ ml); $\Gamma S$ is the total amount of protein adsorbed to the monomolecular film; and $T$ is the total amount of HGL (14.85 μg) or HPL (1 μg) injected under the monomolecular film.

## 3. Results and discussion

### 3.1. Synthesis of various alkylphosphonates (RY)

Alkylphosphonic acid dichloride 2-$R_{4-16}$ synthesis has been easily performed from corresponding *O*-*O*-dimethyl alkylphosphonates 1-$R_{4-16}$ with oxalyl chloride, as described by Marguet et al. (1994), except for compound 2-$R_1$ which has been prepared using classical methods of successive hydrolysis and chlorinating (Scheme 2) (Maier, 1973; Quast et al., 1974). Next, successive and selective substitution of the chlorine atoms of 2-$R_{1-16}$ by various alcohols 3-$Y_{1-16}$ and *p*-nitrophenol in the presence of *N*-methylimidazole (NMI) led to the formation of the desired alkylphosphonates (RY), as depicted in Scheme 2. We thus obtained various *O*-alkyl-*O*-(*p*-nitrophenyl) *n*-undecylphosphonates ($R_{11}Y_{1-16}$) and *O*-undecyl-*O*-(*p*-nitrophenyl) *n*-alkylphosphonates ($R_{1-16}Y_{11}$), with chemical yields ranging from 40 to 70%.

All chiral phosphonates were synthesized in a racemic form. They were purified by silica-gel chromatography. Each enantiomer was then separated by performing chiral liquid chromatography, as described in the experimental section. We decided to define each enantiomer of the same compound by its retention time on chiral HPLC, noted f for 'fast', and s for 'slow'. In the case of ($R_1Y_{11}$) and ($R_4Y_{11}$), since the two respective enantiomers were not separated by chiral HPLC, these two alkylphosphonates were used in a racemic form in the inhibition studies. It also must be noted that for compounds ($R_{11}Y_{1-16}$) there was a sign inversion of the rotatory power between the two enantiomers from ($R_{11}Y_{10}$) to ($R_{11}Y_{16}$).

### 3.2. Forces/area curves of alkylphosphonates (RY)

In order to study the effects of the phosphonates (RY) on the human gastric and pancreatic lipases, we first determined the film stability of all the above compounds and their interfacial properties at the air–water interface. Experiments were performed in the reservoir compartment of the 'zero-order' trough, as described in the experimental section. With all the compounds tested, sharp collapse points are indicative of a high degree of purity. Moreover, the surface-pressure

curves as a function of the molecular area were found to be identical for the two enantiomers of a same compound (Fig. 1). All the films consisting of the previous phosphonates, including ($R_1Y_{11}$) and ($R_{11}Y_1$), in the pure state or mixed with 1,2-dicaprin, were stable with time, i.e. no significant decrease in the surface pressure was observed within 1 h. For the kinetic studies, we selected a surface pressure of $\pi = 20$ mN $m^{-1}$ for mixed inhibitor–1,2-dicaprin films. At this value, which was below the collapse pressure of all the alkylphosphonate (RY) tested, HPL and HGL are active and characterised by linear kinetics when using pure substrate. The covalent inhibition studies of HGL and HPL were then carried out using the monomolecular films technique (Verger and de Haas, 1973; Piéroni and Verger, 1979, 1983; Gargouri et al., 1987).

Fig. 2 shows the variation of the mean area per molecule in mixtures of 1,2-dicaprin with each enantiomer of compounds ($R_{10}Y_{11}$) (Fig. 2, panel A) and ($R_{16}Y_{11}$) (Fig. 2, panel B) at a surface pressure of 18 mN $m^{-1}$. A clear expansion effect on the area per molecule was apparent from the non linear relationship, reflecting a strong deviation from ideality when mixing 1,2-dicaprin and phosphonate inhibitors (Andelman, 1989; Arnett et al., 1989; Pathirana et al., 1992). In each case the deviation from an ideal behavior was less pronounced with the 'fast' enantiomers than with the 'slow' enantiomers. This expansion effect was approximately 11% in a 25:75 1,2-dicaprin–'fast' enantiomer mixture, compared with approximately 22% in a 75:25 1,2-dicaprin–'slow' enantiomer mixture. Furthermore, at various inhibitor molar fractions ($\alpha$): 0.25, 0.50, 0.75, we found (data not shown) collapse pressure values (in mN $m^{-1}$) of: 27.2, 23.4, 21.9 for ($R_{16}Y_{11}$)f and 23.6, 23.1, 21.6 for ($R_{16}Y_{11}$)s, respectively. The corresponding collapse pressure values (in mN $m^{-1}$) were found to be (data not shown): 28.7, 25.4, 22.6 for ($R_{10}Y_{11}$)f and 24.4, 23.4, 22.9 for ($R_{10}Y_{11}$)s, respectively. One can notice that at the working surface pressure of 20 mN $m^{-1}$ all the above mentioned mixed films, consisting of 1,2-dicaprin and phosphonate inhibitors, are stable and thus amenable to be studied by the monomolecular film technique.

Arnett et al. have clearly demonstrated that the chiral recognition in monolayers depends strongly

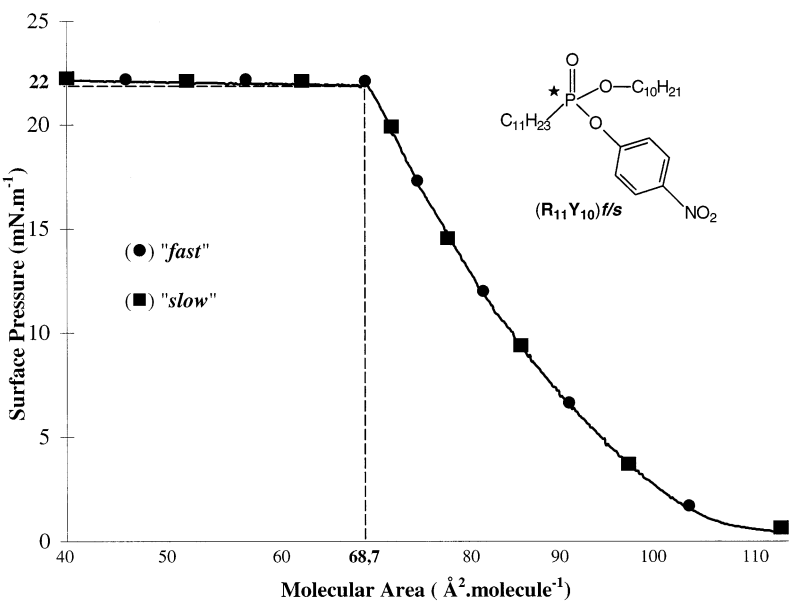


Fig. 1. Surface pressure versus molecular area of monomolecular films of the two enantiomers, 'fast' (■) and 'slow' (●), of the *n*-decyl *p*-nitrophenyl *n*-undecylphosphonate ($R_{11}Y_{10}$).

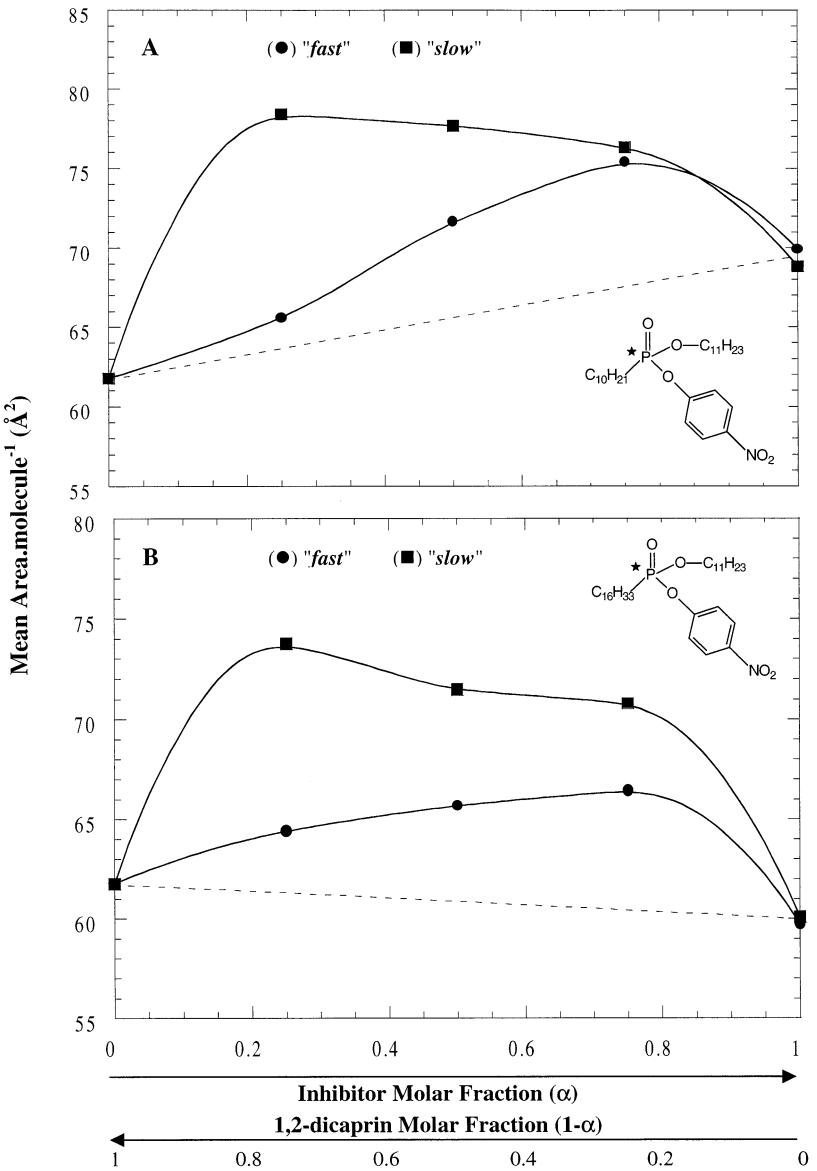


Fig. 2. Mean area per molecule in films formed by mixtures of 1,2-dicaprin with each enantiomer 'fast' (●) and 'slow' (■) of compounds ($R_{10}Y_{11}$) and ($R_{16}Y_{11}$) at a surface pressure of 18 mN $m^{-1}$. The straight dotted lines join the data for the pure compounds indicating ideal mixing.

on the ability of the interacted molecules to bring their chiral centers into favorable stereospecific interactions (Arnett et al., 1989). Such intermolecular effects have been theoretically estimated on simple models by Andelman (1989). Recently, Vodyanoy et al. have detected different diastereomeric interactions of the odorants (+) and (−)-carvone with L−α-1,2-dipalmitoyl-*sn*-glycero-3-phosphocholine (L-DPPC) monolayers (Pathirana et al., 1992). The surface pressure-area isotherms with each enantiomeric carvone show a clear chiral discrimination effect attributed to different packing arrangements of L-DPPC in monolayers exposed to different odorants.

In the case of the two enantiomers of compounds ($R_{10}Y_{11}$) and ($R_{16}Y_{11}$), the differences observed in the mean area per molecule at a constant surface pressure (Fig. 2), disclose diastereomeric interactions of the 'fast' or the 'slow' enantiomer with 1,2-dicaprin in mixed films, regardless of the alkyl chains length ($C_{10}H_{21}$ and $C_{16}H_{33}$).

However, during our investigations, the inhibition studies on HPL and HGL were performed with low molar fraction of compounds (RY) which were found to be very efficient inhibitors (vide infra). When using very low concentrations of 'fast' or 'slow' alkylphosphonate compound in mixed films with 1,2-dicaprin, the molar fraction of the inhibitor is very close to the relative surface occupied by each component. In these conditions, the alkylphosphonate enantiomers will not deviate too much from the additivity rule of their respective area per molecule. Their inhibitory power can then be expressed as the function of the molar fractions of the inhibitor relative to the inhibitor plus 1,2-dicaprin.

### *3.3. HGL and HPL activities on mixed films containing alkylphosphonates*

Lipase activities were measured as a function of the inhibitor molar fraction ($\alpha$). With both lipases tested, the hydrolysis of 1,2-dicaprin decreased sharply as the molar fraction of inhibitors (RY) increased. Fig. 3 showed the variation, as a function of the alkyl R or ester Y chain length, of the inhibitor molar fraction ($\alpha_{50}$), which reduced enzyme activity to 50% of its initial value on pure 1,2-dicaprin.

With the two lipases, there is no obvious correlation between $\alpha_{50}$ and the chain length, R or Y. In the case of HPL (Fig. 3, panel A), compounds ($R_{11}Y_{1-16}$)s and ($R_{1-16}Y_{11}$)s, with higher retention times on chiral HPLC, are the most potent inhibitors. Moreover, between the above two series of 'slow' enantiomers, the best inhibitors of HPL are ($R_{11}Y_{16}$)s and ($R_{16}Y_{11}$)s. On the contrary, in the case of HGL (Fig. 3, panel B), no clear distinction could be made between the 'slow' or the 'fast' enantiomers. The best inhibition of HGL is obtained with compounds including alkyl and ester chains length from four to eight carbon atoms. This result confirms the known preference of HGL for medium and short lipid chains (Rogalska et al., 1990, 1995).

HPL and HGL stereoprefence for compounds (RY) was then studied on the basis of a new parameter, the stereoselectivity index (S.I.) (39, 40) as defined in Eq. (1):

$$\text{S.I. } (\%) = \left|\frac{\alpha_{50}\text{f} - \alpha_{50}\text{s}}{\alpha_{50}\text{f} + \alpha_{50}\text{s}}\right| \cdot 100 \quad (1)$$

where $\alpha_{50}$f and $\alpha_{50}$s are the molar fraction of the 'fast' and 'slow' enantiomers of the same compound, respectively. Fig. 4 shows the variation of S.I. values as a function of the dissymmetry between the alkyl and the ester chain length, for compounds ($R_{11}Y_n$) and ($R_nY_{11}$), with $n$ ranging from six to 16 carbon atoms. This new parameter called the dissymmetry index (D.I.) was calculated as follows:

$$\text{D.I.} = (n - 11) \text{ with } n \text{ varying from six to 16 carbon atoms} \quad (2)$$

With HPL (Fig. 4, panel A), all compounds presented S.I. values higher than 40%, indicating a significant chiral discrimination between two enantiomers. Moreover, the highest values ($\sim$ 87%) were reached for D.I. values equal to $+1$ and $+5$; showing a preference of HPL for compounds ($R_{11}Y_{12}$) and ($R_{16}Y_{11}$), respectively. In contrast to HPL, HGL (Fig. 4, panel B) shows a strong dependency of S.I. values as a function of D.I. values. The greatest stereoselectivity is observed for a D.I. value equal to $-1$, corresponding to the compounds ($R_{11}Y_{10}$) and ($R_{10}Y_{11}$).

From the data presented in Fig. 4, one can also notice that there is a negligible chemoselective discrimination in the lipases active site between the isosteric methylene group ($-CH_2-$) of an alkylphosphonate chain and the alkoxy group ($-OCH_2-$) of an ester phosphonic chain; since a permutation between R and Y chains does not strongly affect the S.I. values. A molecular interpretation of the above data has to wait for the resolution of the three dimensional structures of lipase-phosphonate complexes.

Further experiments were carried out with the best inhibitors: compounds ($R_{11}Y_{16}$) and ($R_{16}Y_{11}$) on HPL, and compounds ($R_{11}Y_{10}$) and ($R_{10}Y_{11}$) on HGL. The 'slow' enantiomers of these alkylphosphonates were in fact the best inhibitors of the digestive lipases (Fig. 3 and Table 1). Moreover, these compounds displayed the highest S.I. values (see Fig. 4).

We first determined the influence of the enantiomeric excess (*ee*) on the inhibitory power ($\alpha_{50}$) (Fig. 5). In three cases, an hyperbolic relationship was observed. However, no significant

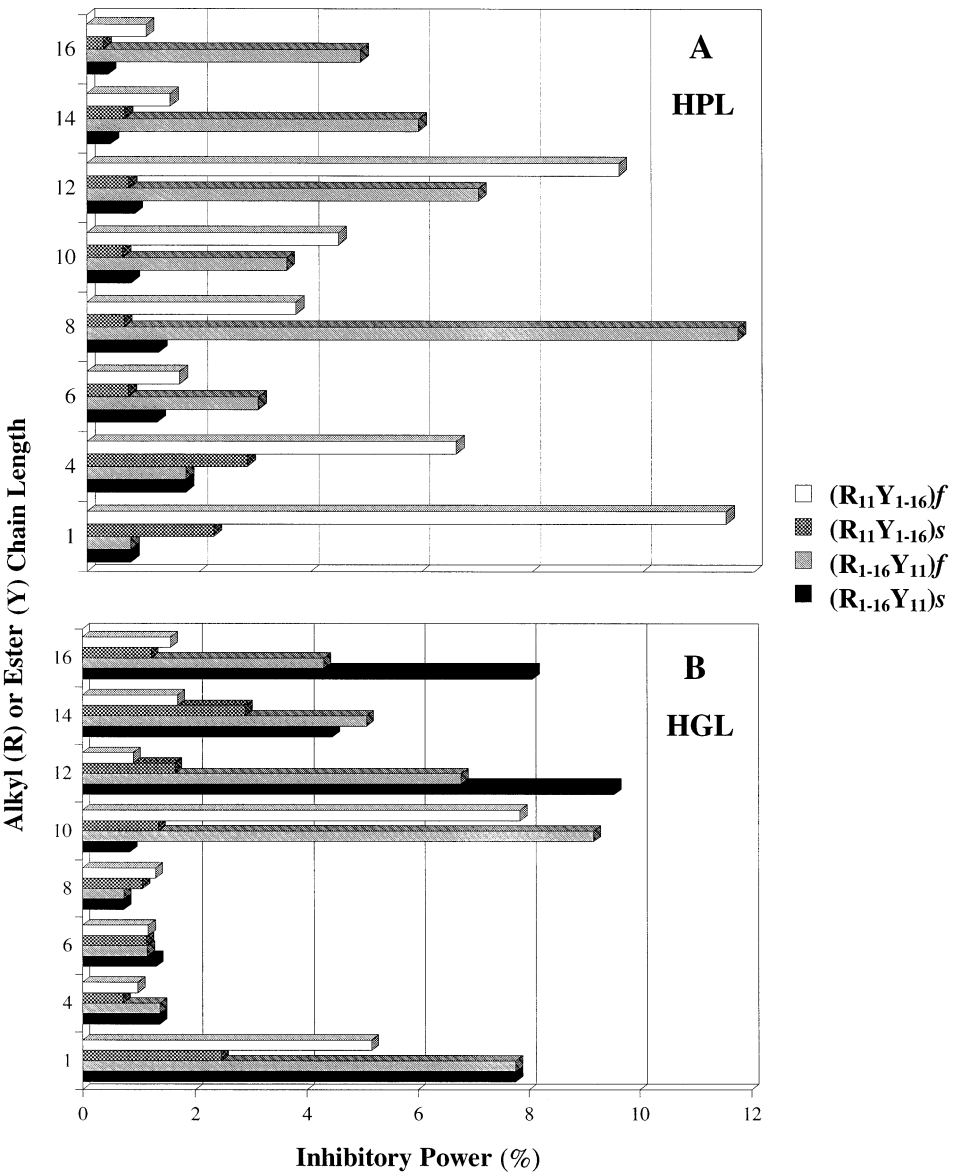


Fig. 3. Variation of the inhibitor molar fraction $\alpha_{50}$ (%), reducing HPL (panel A) or HGL (panel B) activity to 50% of its initial value on 1,2-dicaprin during monolayer experiments at $\pi = 20$ mN m$^{-1}$, as a function of the alkyl (R) or ester (Y) chain length, for compounds ($R_{11}Y_{1-16}$) and ($R_{1-16}Y_{11}$).

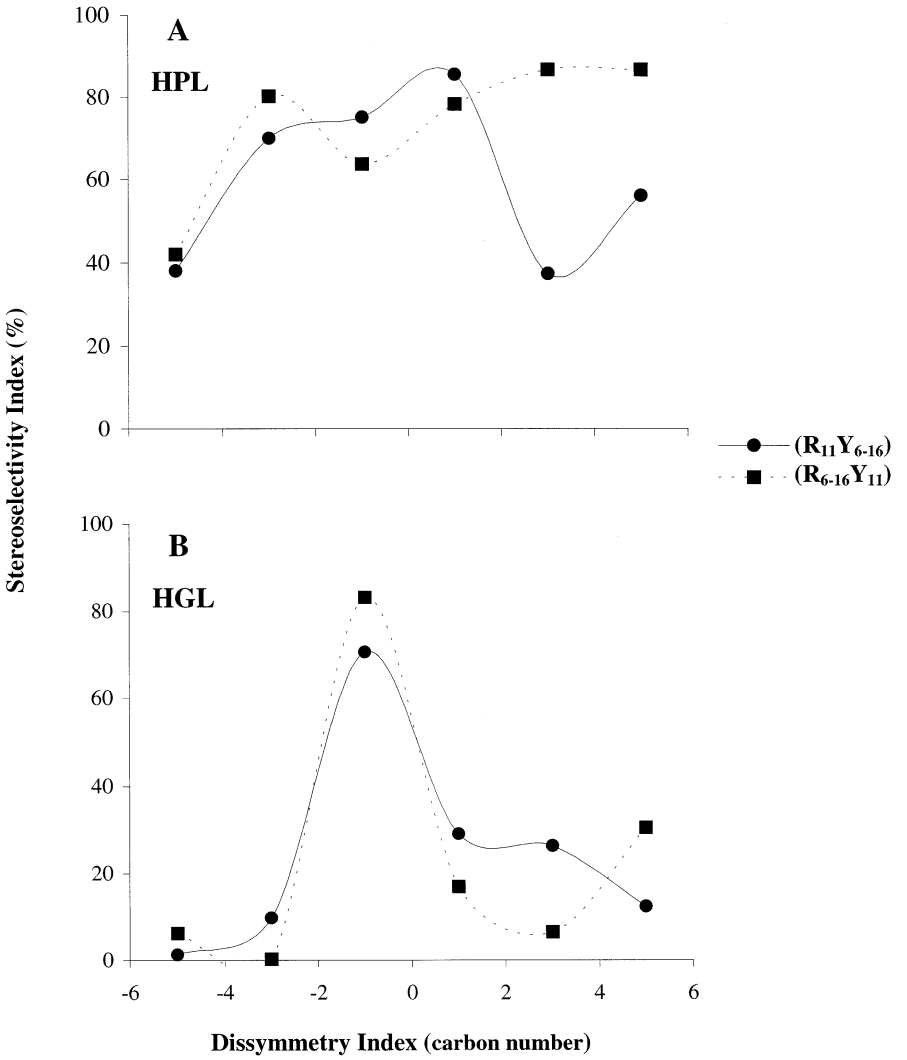


Fig. 4. Variation of the S.I. (%), as a function of the dissymmetry index (D.I.), with alkylphosphonates ($R_{11}Y_{1-16}$) and ($R_{1-16}Y_{11}$), on HPL (panel A) or HGL (panel B). The lipases enantioselectivity for these compounds was studied on the basis of new parameters, the S.I. define by analogy with the enantiomeric excess, and the D.I. showing the dissymmetry between the alkyl and the ester chains length:

$$\text{S.I.} \quad (\%) = \left|\frac{\alpha_{50}\text{f} - \alpha_{50}\text{s}}{\alpha_{50}\text{f} + \alpha_{50}\text{s}}\right| \cdot 100$$

and D.I. $= (n - 11)$ with $n$ ranging from six to 16 carbon atoms.

variation of $\alpha_{50}$ was observed for *ee* values above $-50\%$.

Furthermore, HPL and HGL superficial concentrations at the lipidic interface were then quantified by means of ELISA tests (Aoubala et al., 1995). The latter method was developed at our laboratory in order to measure the surface density of lipases in the picogram range (Aoubala et al., 1995). The recovery levels of each lipase injected under the lipid monomolecular films were as high as 90% for HPL and 80% for HGL (see supplementary material for details). As the monolayer

system is characterised by a low specific surface (around 1 $cm^2$ $cm^{-3}$), only a small fraction of the total amount of enzyme is actually bound to the monomolecular film. In the particular cases of HPL and HGL, using the four above cited inhibitors, less than 0.7% (HPL) and 0.2% (HGL) of the total amount of injected lipase, were recovered after film aspiration (see supplementary material for details). Judging from this percentage of film-bound enzyme, the effective interfacial stoichiometry at the $\alpha_{50}$ inhibitor molar fraction can be calculated and their values are reported in Table 2: one molecule of HGL, bound to a mixed monomolecular film, could statistically interact with $1.4 \times 10^4$ substrate molecules, and was inhibited at 50% of its initial rate on 1,2-dicaprin by 110 molecules of inhibitor $(R_{10}Y_{11})$s. In the case of HPL, one molecule of this enzyme could statistically interact with $5.9 \times 10^4$ substrate molecules, and was inhibited at 50% of its initial rate on 1,2-dicaprin by 153 molecules of inhibitor $(R_{11}Y_{16})$s. Concerning THL, its inhibitory power ($\alpha_{50}$) on HPL is $1.5 \times 10^{-4}$%, which is 2000 times higher than the best alkylphosphonate enantiomer (data not shown). With HGL (Ransac et al., 1991), the value of THL inhibitory power (0.25%) is quite close to the value obtained in our study with compound $(R_{10}Y_{11})$s.

Fig. 6 (HPL) and Fig. 7 (HGL) show the variations of the residual activity (%) and the superficial concentration, $\Gamma$ (%), as a function of the inhibitor molar fraction ($\alpha$). In each case, a decrease in the enzyme surface density was systematically observed as the molar fraction of inhibitors increased. In the case of HPL, the binding curves obtained with each enantiomer were comparable. Moreover, we showed that at a given inhibitor molar fraction ($\alpha = 15\%$), the variation of the superficial concentration of HPL ($\Gamma = 37.1$, 35.9, 36.7, 39.5, 40.3, 37.8, 38.2%) did not depend on the enantiomeric excess ($ee = -100$, $-96$, $-80$, $-50$, 0, $+50$, $+100$%, respectively) of inhibitor $(R_{16}Y_{11})$.

With compounds $(R_{11}Y_{16})$f, $(R_{11}Y_{16})$s and $(R_{16}Y_{11})$s on HPL (Fig. 6) and compounds $(R_{11}Y_{10})$s and $(R_{10}Y_{11})$s on HGL (Fig. 7), we observed a clear difference between the inhibition and the binding curves as a function of $\alpha$. On the contrary, with compound $(R_{16}Y_{11})$f on HPL (Fig. 6) and compounds $(R_{11}Y_{10})$f and $(R_{10}Y_{11})$f on HGL (Fig. 7), the inhibition and binding curves are nearly superimposed.

These differences between the inhibition and interfacial behavior are well illustrated by the ratio between the molar fraction leading to half lipase binding ($\Gamma_{50}$), to the $\alpha_{50}$ inhibitor molar fraction (Table 1). The highest values of this ratio, $\Gamma_{50}/\alpha_{50}$ correspond to the most potent enantiomeric alkylphosphonate inhibitors.

### 3.4. Kinetic model of the covalent inhibition of a lipolytic enzyme at a lipid–water interface by two enantiomeric compounds

The kinetic model presented in Fig. 8 has been developed to describe the covalent inhibition of

Table 1
Values of the inhibitory power, $\alpha_{50}$ (%), lipases superficial concentration, $\Gamma_{\alpha_{50}}$ (%) (expressed as the ratio of the amount of lipase adsorbed on each pure enantiomeric inhibitor at the $\alpha_{50}$ molar fraction, to the total amount of lipase adsorbed on 1,2-dicaprin films), and inhibitor molar fraction, $\Gamma_{50}$, leading to half lipase adsorption[a]

| | HPL | | | | HGL | | | |
|---|---|---|---|---|---|---|---|---|
| | $(R_{11}Y_{16})$ | | $(R_{16}Y_{11})$ | | $(R_{11}Y_{10})$ | | $(R_{10}Y_{11})$ | |
| | Fast | Slow | Fast | Slow | Fast | Slow | Fast | Slow |
| $\alpha_{50}$ | 1.2 | 0.3 | 4.9 | 0.4 | 7.8 | 1.4 | 9.2 | 0.8 |
| $\Gamma_{\alpha_{50}}$ | 90.0 | 99.8 | 58.7 | 99.4 | 43.7 | 80.0 | 36.7 | 93.1 |
| $\gamma_{50}$ | 8.9 | 12.3 | 5.0 | 12.3 | 4.9 | 4.2 | 4.1 | 31.0 |
| $\gamma_{50}/\alpha_{50}$ | 7.4 | 41.0 | 1.0 | 30.8 | 0.6 | 3 | 0.4 | 38.8 |

[a] These data were determined during inhibition studies and ELISA tests with mixed films inhibitor–1,2-dicaprin at $\pi = 20$ mN $m^{-1}$ for compounds $(R_{11}Y_{16})$ and $(R_{16}Y_{11})$ on HPL at pH 8, and compounds $(R_{11}Y_{10})$ and $(R_{10}Y_{11})$ on HGL at pH 5.

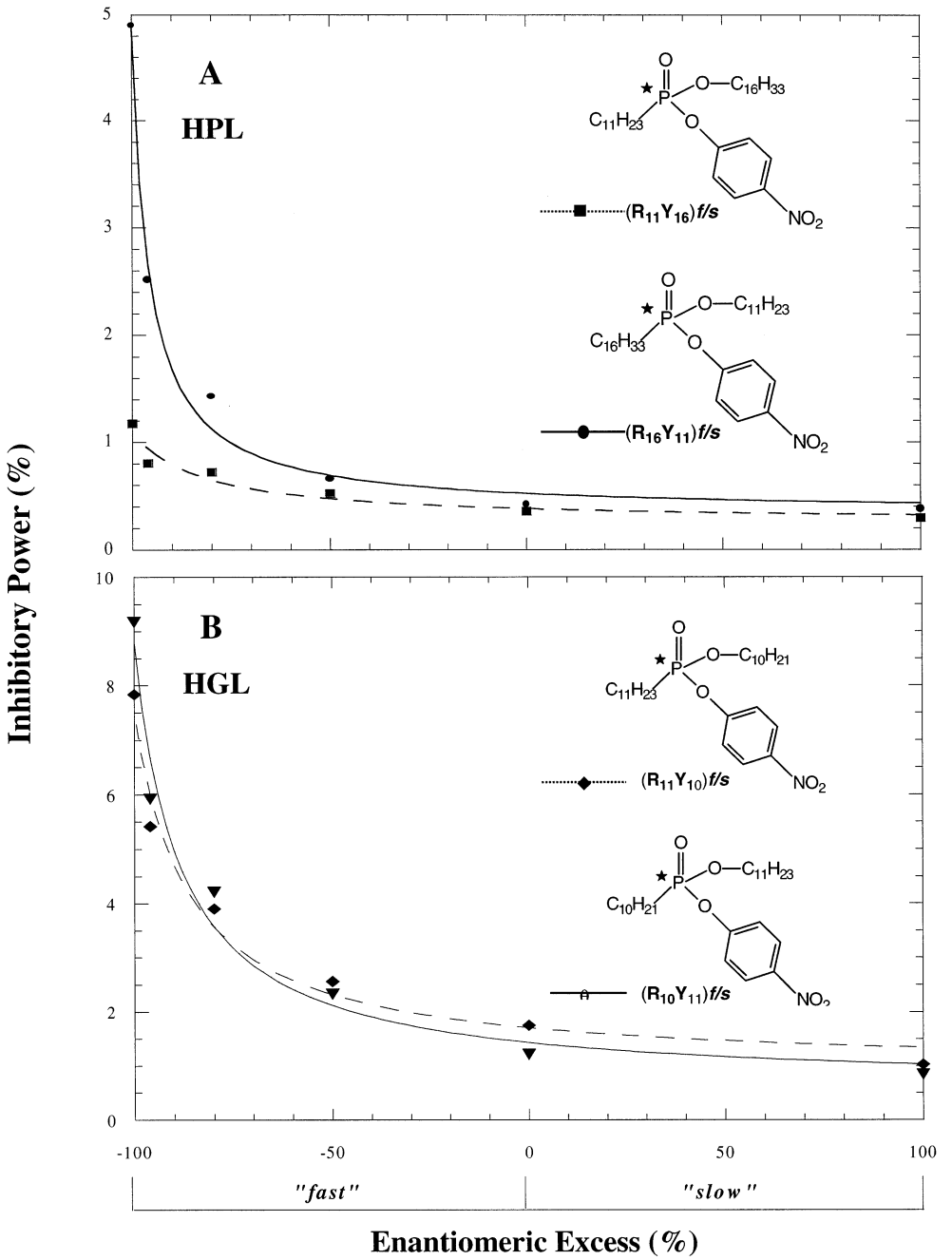


Fig. 5. Variation of the inhibitory power $\alpha_{50}$ (%) as a function of the enantiomeric excess *ee* (%) of compound ($R_{11}Y_{16}$) or ($R_{16}Y_{11}$) on HPL (panel A) and compound ($R_{11}Y_{10}$) or ($R_{10}Y_{11}$) on HGL (Panel B), in mixed films inhibitor–1,2-dicaprin at $\pi = 20$ mN m$^{-1}$ using the monomolecular films technique.

Table 2
Interfacial stoichiometry values, at $\pi = 20$ mN m$^{-1}$, by mole of enzyme HPL or HGL, at the $\alpha_{50}$ inhibitor molar fraction, for each enantiomer of compounds ($R_{11}Y_{16}$) and ($R_{16}Y11$) with HPL, and ($R_{11}Y_{10}$) and ($R_{10}Y_{11}$) with HGL

| | Per HGL molecule | | Per HGL molecule | |
|---|---|---|---|---|
| | Fast | Slow | Fast | Slow |
| 1,2-dicaprin | $1.4 \times 10^4$ | | $5.9 \times 10^4$ | |
| ($R_{11}Y_{10}$) | 1080 | 162 | – | – |
| ($R_{10}Y_{11}$) | 1200 | 110 | – | – |
| ($R_{11}Y_{16}$) | – | – | 616 | 153 |
| ($R_{16}Y_{11}$) | – | – | 2771 | 210 |

lipolytic enzymes at a lipid–water interface, by two enantiomeric inhibitors ($I_R$) and ($I_S$), with the formation of two different forms of covalently inhibited enzyme ($E^*i_R$) and ($E^*i_S$). In this model, we assume that the enzyme binding step at the lipidic interface ($E \rightleftharpoons E^*$) is slow as compared to the three other reversible equilibria, involving the substrate or the inhibitors. The kinetic treatment of this new model was developed by analogy with the previous analysis by Ransac et al. (1990, 1991). In the above kinetic treatment, the inhibitor was assumed to be in large molar excess as compared to the adsorbed enzyme. This assumption was experimentally checked to be fulfilled (see Table 2).

The sigmoidal expression of the time dependence of product released ($P$), normalized with the enantiomeric excess ($ee$) and the inhibitor molar fraction ($\alpha$) is:

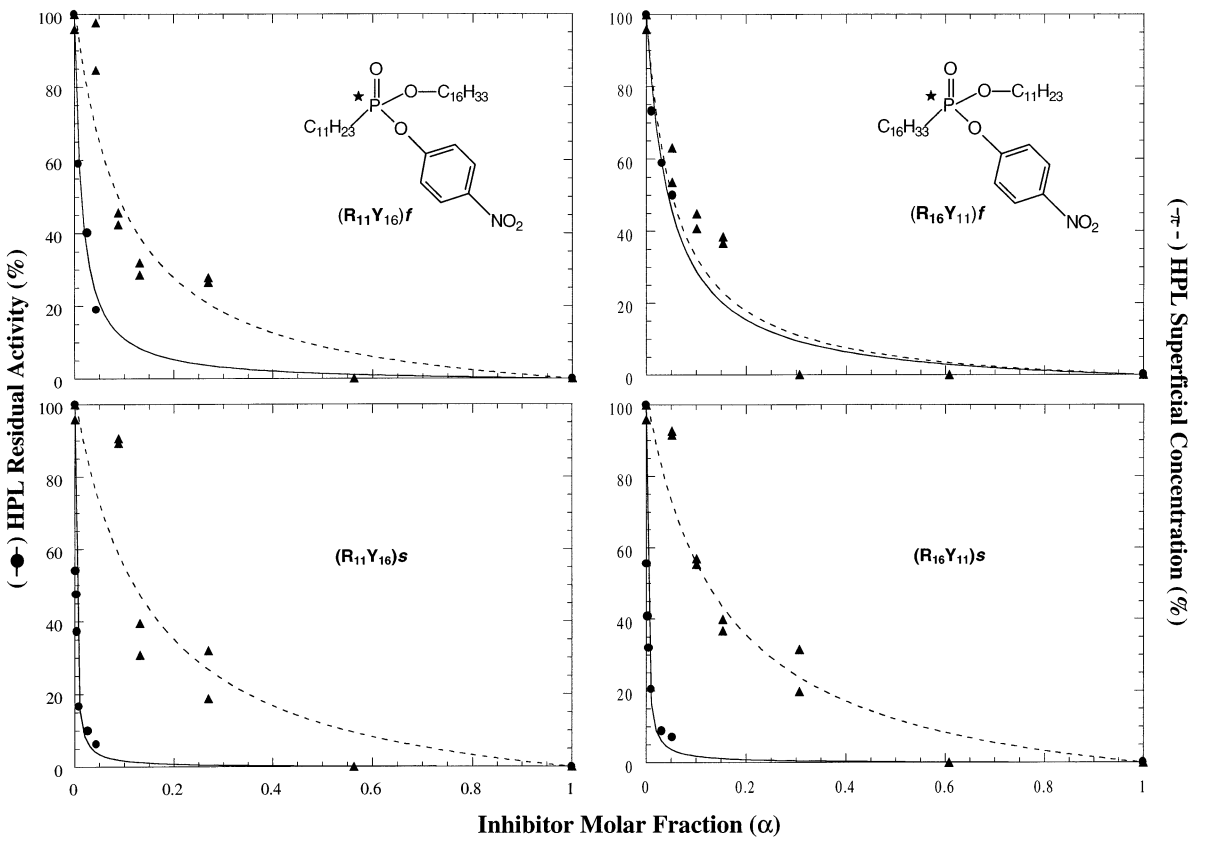


Fig. 6. Variation of HPL residual activity (%) (—) and superficial concentration (%) (----) as a function of inhibitors molar fraction, ($R_{11}Y_{16}$) or ($R_{16}Y_{11}$). HPL final concentration 19.4 ng ml$^{-1}$ in the sub-phase at pH 8, surface pressure 20 mN m$^{-1}$.

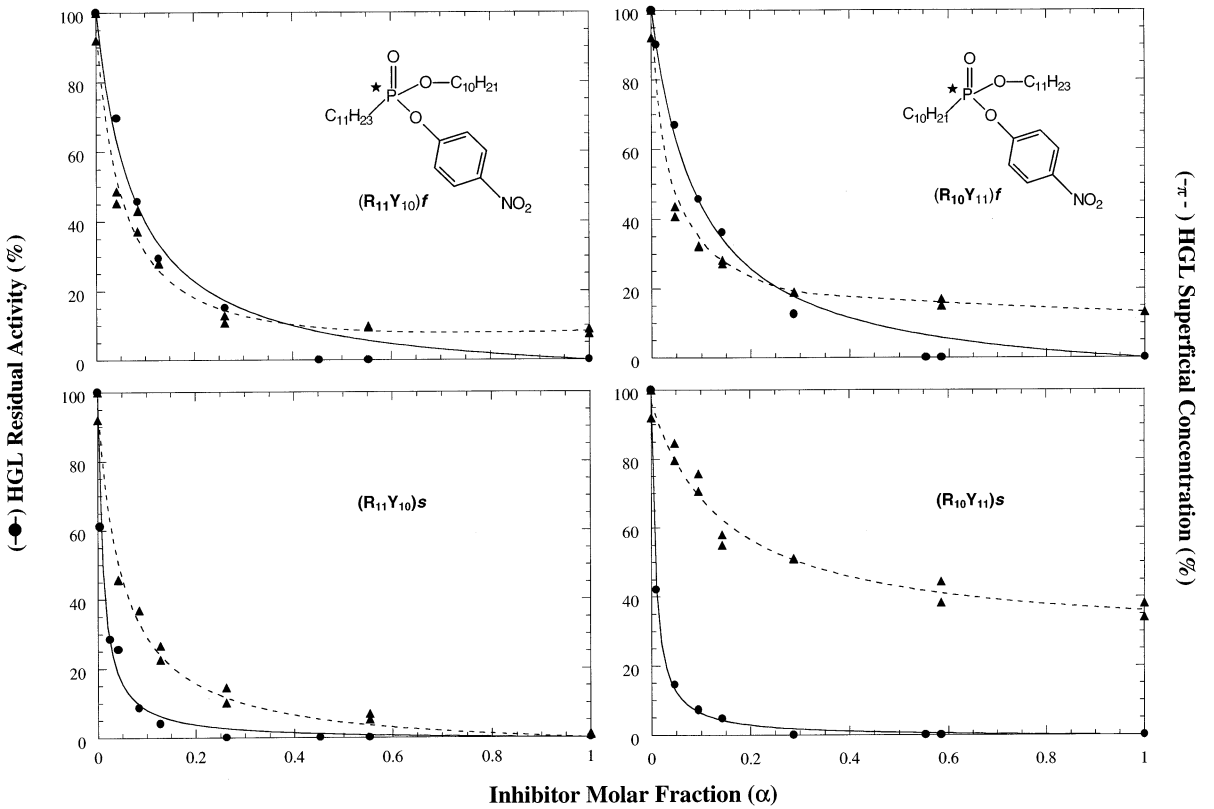


Fig. 7. Variation of HGL residual activity (%) (—) and Superficial Concentration (%) (----) as a function of inhibitors molar fraction, ($R_{11}Y_{10}$) or ($R_{10}Y_{11}$). HGL final concentration 288.4 ng ml$^{-1}$ in the sub-phase at pH 5, surface pressure 20 mN m$^{-1}$.

$$P = \frac{1-\alpha}{\alpha} \cdot \frac{2}{Ks \cdot (1+ee) + Kf \cdot (1-ee)} \cdot \left[1 - \frac{\tau_1 \cdot e^{-t/\tau_1} - \tau_2 \cdot e^{-t/\tau_2}}{\tau_1 - \tau_2}\right] \quad (3)$$

with

$$E_0 \cdot Ks = \frac{k_{i_S}}{K^*_{I_S}} \cdot \frac{K^*_M}{k_{cat}}, \quad E_0 \cdot Kf = \frac{k_{i_R}}{K^*_{I_R}} \cdot \frac{K^*_M}{k_{cat}},$$

$$\alpha = \frac{I_R + I_S}{I_R + I_S + S}, \quad ee = \frac{I_S - I_R}{I_R + I_S}$$

$E_0Ks$ (for the 'slow' enantiomer) and $E_0Kf$ (for the 'fast' enantiomer) represent the ratio of the specificity constant $k_i/K^*_I$ of each enantiomeric inhibitor to the specificity constant of the substrate $k_{cat}/K^*_M$. The kinetic significance of these constants, $E_0Ks$ and $E_0Kf$, is in fact the relative reactivity as well as the relative affinity of one inhibitor as compared to the substrate. Furthermore, $\frac{Ks}{Kf} = \left(\frac{k_{i_S}}{K^*_{I_S}}\right) \cdot \left(\frac{K^*_{I_S}}{k_{i_R}}\right)$ characterizes the ratio of the specificity constants of the two enantiomeric inhibitors ($I_R$) and ($I_S$).

$\tau_1$ and $\tau_2$ are complex parameters (see supplementary material for details) including $k_d$, $k_p$, $ki_S$, $ki_R$, $K^*_M$, $K^*I_S$, $K^*I_R$ and represent the time constants of the combined partial reversible reactions ($E \rightleftharpoons E^*$) ($E^* + S \rightleftharpoons E^*S \rightleftharpoons E^*S$) ($E^* + I_S \rightleftharpoons E^*I_S$) ($E^* + I_R \rightleftharpoons E^*I_R$), as well as the irreversible reactions ($E^*I_S \rightarrow E^*i_S$) and ($E^*I_R \rightarrow E^*i_R$).

The corresponding equation of the enzymatic velocity is:

$$v = \frac{dP}{dt} = \frac{1-\alpha}{\alpha} \cdot \frac{2}{Ks \cdot (1+ee) + Kf \cdot (1-ee)} \cdot \frac{e^{-t/\tau_1} - e^{-t/\tau_2}}{\tau_1 - \tau_2} \quad (4)$$

As can be seen from Eq. (4), the enzyme velocity possesses a maximal value, $v_{\text{inflexion}}$ (Eq. (5)) at a given time $t_{\text{inflexion}}$ (Eq. (6)) which correspond to the inflexion point of the experimental kinetic curve of the product release as a function of time.

$$v_{\text{inflexion}} = \frac{dP}{dt} = \frac{1-\alpha}{\alpha} \cdot \frac{2}{Ks \cdot (1+ee) + Kf \cdot (1-ee)} \cdot \frac{1}{\tau_1} \cdot \left(\frac{\tau_2}{\tau_1}\right)^{\frac{\tau_2}{\tau_1-\tau_2}} \quad (5)$$

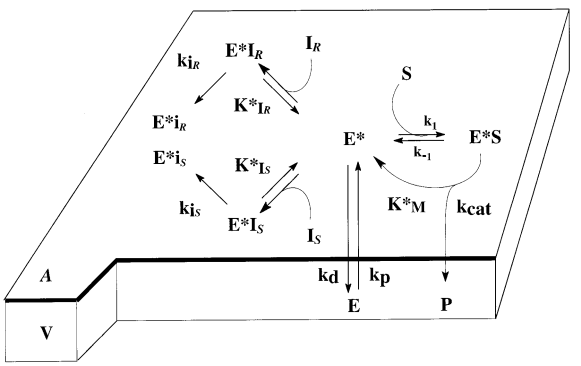


Fig. 8. Kinetic model illustrating the covalent inhibition of a lipolytic enzyme at a lipid–water interface. Symbols and abbreviations are as follows: $A$, total interfacial area (surface); $V$, total volume (volume); $E_0$, total enzyme concentration (molecule/volume); $E$, free enzyme concentration (molecule/volume); $E^*$, interfacial enzyme concentration (molecule/surface); $S$, interfacial concentration of substrate (molecule/surface); $I_R$, interfacial concentration of inhibitor-($R$) (molecule/surface); $I_S$, interfacial concentration of inhibitor-($S$) (molecule/surface); $P$, product concentration (molecule/volume); $E^*S$, interfacial enzyme-substrate complex concentration (molecule /surface); $E^*I_R$, interfacial enzyme-inhibitor-($R$) complex concentration (molecule/surface); $E^*I_S$, interfacial enzyme–inhibitor-($S$) complex concentration (molecule/surface); $E^*i_R$, interfacial enzyme covalently inhibited by inhibitor-($R$) concentration (molecule/surface); $E^*i_S$, interfacial enzyme covalently inhibited by inhibitor-($S$) concentration (molecule/surface); $k_d$, desorption rate constant ($\text{time}^{-1}$); $k_p$, penetration rate constant (volume surface$^{-1}$ $\text{time}^{-1}$); $k_1$, rate constant (surface molecule$^{-1}$ $\text{time}^{-1}$); $k_{-1}$, rate constant ($\text{time}^{-1}$); $k_{cat}$, catalytic rate constant ($\text{time}^{-1}$); $k_{i_R}$, inhibition rate constant for the enzyme–inhibitor-($R$) complex ($\text{time}^{-1}$); $k_{i_S}$, inhibition rate constant for the enzyme–inhibitor-($S$) complex ($\text{time}^{-1}$); $K^*_M$, interfacial Michaëlis–Menten constant (molecule/surface); $K^*_{I_R}$, interfacial dissociation constant for the enzyme-inhibitor-($R$) complex (molecule/surface); $K^*_{I_S}$, interfacial dissociation constant for the enzyme-inhibitor-($S$) complex (molecule/surface).

$$t_{\text{inflexion}} = \frac{\ln \tau_1 - \ln \tau_2}{\tau_1 - \tau_2} \cdot \tau_1 \cdot \tau_2 \quad (6)$$

On the basis of this new model, and starting from Eq. (3), we performed curve fitting on 20 experimental kinetics obtained with HPL, using each of the following enantiomers ($R_{11}Y_{10}$), ($R_{11}Y_{16}$) and ($R_{16}Y_{11}$). In a first step, we fitted each kinetic experiment, $P = f(t)$, and in a second step we calculated by an iteration method the values of $Kf$, $Ks$, $\tau_1$, $\tau_2$ as a function of $ee$, using MicroMath Scientist® for Windows™ v. 2.01 software.

It must be noted that $\tau_1$ and $\tau_2$ depend on both substrate ($S$), inhibitor ($I$) concentrations and on the enantiomeric excess ($ee$). In order to fit our experimental curves, $P = f(t)$, we intentionally decided to keep constant the two parameters, $\tau_1$ and $\tau_2$ for a given compound.

The classification of the inhibitors according to the theoretical values of $E_0Ks$ and $E_0Kf$ obtained (Table 3) is in agreement with the classification of the inhibitory power ($\alpha_{50}$), previously established with HPL (Fig. 3, panel A):

$$(R_{11}Y_{16})s > (R_{16}Y_{11})s > (R_{11}Y_{10})s > (R_{11}Y_{16})f > (R_{11}Y_{10})f > (R_{16}Y_{11})f$$

Starting from the calculated values of the parameters listed in Table 3, in the case of compounds ($R_{11}Y_{16}$) and ($R_{16}Y_{11}$) with HPL (see supplementary material for details), we found an hyperbolic dependency of the $\alpha_{50}$ values as a function of the enantiomeric excess, in good agreement with the experimental data presented in Fig. 5.

### *3.5. Kinetic model of the pseudo-competitive inhibition of a lipolytic enzyme at a lipid–water interface by two enantiomeric compounds*

In order to simplify the kinetic treatment of the general covalent inhibition model presented in Fig. 8, we can assume as a first approximation that HGL and HPL inhibition with alkylphosphonates (RY), is pseudo-competitive; i.e. the rate constants ($k_{i_R}$, $k_{i_S}$) are slow and negligible as compared to $k_{cat}$. This approximation is based on the experimental observation that after the inflex-

Table 3
Results of the curve fitting on 20 experimental kinetic curves registered on HPL, with each enantiomer of the compounds ($R_{11}Y_{10}$), ($R_{11}Y_{16}$) and ($R_{16}Y_{11}$), using MicroMath Scientist® for Windows™ v. 2.01 software

| | $E_0Kf$ ($\times 10^{14}$) | $E_0Ks$ ($\times 10^{14}$) | $\tau_1$ (min) | $\tau_2$ (min) | $\frac{K_s}{K_f}=\left(\frac{k_{i_s}}{K_{I_s}}\right)\cdot\left(\frac{K^*_{I_R}}{k_{i_R}}\right)$ |
|---|---|---|---|---|---|
| ($R_{11}Y_{10}$) | 0.28 | 2.61 | 1.1 | 35.6 | 9.3 |
| ($R_{11}Y_{16}$) | 1.26 | 2.80 | 2.0 | 56.1 | 2.2 |
| ($R_{16}Y_{11}$) | 0.21 | 2.73 | 1.0 | 84.2 | 13.0 |

ion point, the decline with time of the recorded kinetic curves is rather slow, reflecting qualitatively a slow irreversible covalent reaction process.

Eq. (7) describes the steady-state velocity under monolayer conditions in the case of this pseudo-competitive model.

$$v=\frac{dP}{dt}=k_{cat}\cdot E_0\cdot \frac{S}{K^*_M\left(1+\frac{I_R}{K^*_{I_R}}+\frac{I_S}{K^*_{I_S}}+\frac{k_d}{k_p\cdot {}^{A}/_{V}}\right)+S} \quad (7)$$

Using this latter equation we defined $R_v$ as the ratio of steady-state velocities:

$R_v$ = (velocity in the presence of an inhibitor with $K^*_I = K^*_M$)/(velocity in the presence of an inhibitor with $K^*_I \neq K^*_M$).

Starting from Eq. (7), the relationship between $R_v$ and the inhibitor molar fraction ($\alpha$) and the enantiomeric excess ($ee$), can be described as follows:

$$R_v = 1+\alpha\cdot\frac{B\cdot(ee+1)-1}{A} \quad (8)$$

With

$$A = K^*_M\cdot A_S\cdot\left(1+\frac{k_d}{k_p\cdot {}^{A}/_{V}}\right)+1$$

$$B=\frac{1}{2}\cdot\left[\frac{K^*_M}{K^*_{I_S}}-\frac{K^*_M}{K^*_{I_R}}\right]$$

The relationship between $\alpha_{50}$ and $ee$ (Eq. (9)) was deduced from Eq. (8) by analogy with the kinetic treatment of Ransac et al. in the case of competitive kinetic model with two inhibitors (Ransac et al., 1990).

$$\alpha_{50}=\frac{A}{B\cdot ee+(B+2\cdot A-1)} \quad (9)$$

This hyperbolic dependency is in agreement with the experiments presented in Fig. 5. In all cases, the value of, $A = K^*_M\cdot A_S\cdot(1+k_d/(k_p\cdot A/V))+1$ was found equal to 1, indicative of a very low amount of adsorbed enzyme in the lipid monolayer ($k_d/(k_p\cdot A/V)$), as well as a low value of $K^*_M$ as compared to the interfacial substrate concentration ($1/A_S$) . Unfortunately, the calculated values of $B$ can not be simply interpreted since they reflect the difference between the ratio of the interfacial Michaëlis–Menten constant to the inhibitor dissociation constants (Eq. (8)).

In order to simplify the interpretation of the calculated constants, we consider the case of one inhibitor ($I$). The rearrangement of Eq. (7), gives the following hyperbolic expression of the lipase residual activity:

$$\text{Lipase residual activity (\%)}=\frac{v}{k_{cat}\cdot E_0}=\frac{1-\alpha}{\alpha\cdot B'+A} \quad (10)$$

With

$$A = K^*_M\cdot A_S\cdot\left(1+\frac{k_d}{k_p\cdot {}^{A}/_{V}}\right)+1,$$

$$B' = \left(\frac{K^*_M}{K^*_I} - 1\right)$$

The curve fitting of the experimental data presented on Figs. 6 and 7, using Eq. (10), allows us to estimate the value of the ratio $K^*_M/K^*_I$ for each enantiomer of the compounds ($R_{11}Y_{16}$) and ($R_{16}Y_{11}$) with HPL, and the compounds ($R_{11}Y_{10}$) and ($R_{10}Y_{11}$) with HGL (Table 4). In the case of the 'fast' enantiomers, the small values of the ratio, $K^*_M/K^*_I$, confirm their low inhibitory power (see Fig. 3). Contrary to compounds ($R_{11}Y_{16}$)*s* and ($R_{16}Y_{11}$)*s* which display differential inhibitory powers with HPL and HGL, compounds ($R_{11}Y_{10}$)*s* and ($R_{10}Y_{11}$)*s* have similar values of $K^*_M/K^*_I$ with both lipases.

When we are dealing with powerful inhibitors, i.e. with low $\alpha_{50}$ values, minimal changes in the interfacial excess of enzyme is to be expected in the presence or absence of the inhibitor, if one assumes that the global 'interfacial quality' is not significantly affected by small proportions of inhibitors. Indeed, in the case of HPL and HGL, the superficial concentrations ($\Gamma_{\alpha_{50}}$) at the $\alpha_{50}$ molar fractions of inhibitors ($R_{11}Y_{16}$)s and ($R_{16}Y_{11}$)s, and ($R_{11}Y_{10}$)s and ($R_{10}Y_{11}$)s is close to 100% (Table 1).

By definition, the ratio of the two interfacial kinetic constants ($K^*_M/K^*_I$) can be expressed as:

$$\frac{K^*_M}{K^*_I} = \left(\frac{[E^*]\cdot[S]}{[E^*S]}\right)\cdot\left(\frac{[E^*I]}{[E^*]\cdot[I]}\right) \quad (11)$$

If we assume that the enzyme partitioning equilibrium ($E \rightleftharpoons E^*$), is not affected by the presence of the inhibitor (see Table 1 and Figs. 6 and 7), at the $\alpha_{50}$ molar fraction we have $[E^*S] = [E^*I]$, and Eq. (11) can be rewritten as Eq. (12):

$$\frac{K^*_M}{K^*_I} = \frac{[S]}{[I]} \quad (12)$$

One can notice that this simplified expression of $K^*_M/K^*_I$ is comparable to the reverse value of $\alpha_{50}$, that is to say: $(S + I/I)$.

In the case of the 'slow' enantiomers, the interfacial stoichiometry (Table 2) has been calculated. We can thus deduce the values of the ratio, $K^*_M/K^*_{I_S}$, by simply dividing the amount of substrate by the amount of the 'slow' enantiomer, at the $\alpha_{50}$ molar fraction.

With HPL this ratio was then estimated as 386 and 281 for ($R_{11}Y_{16}$)s and ($R_{16}Y_{11}$)s, respectively. In the case of HGL, this ratio was estimated to be 86 and 127 for ($R_{11}Y_{10}$)s and ($R_{10}Y_{11}$)s, respectively (see Table 4). The obtained values with the 'slow' enantiomers are in good agreement with the values calculated from Eq. (10) (see Table 4), corroborating thus the assumption that the enzyme partitioning equilibrium is not affected by the presence of these inhibitors.

If we assume that $k_{cat}$ is small as compared to $k_{-1}$ (Fig. 8), we can as usual assimilate $K^*_M$ as the interfacial dissociation constant of the ($E^*S$) complex. With this assumption, the ratio $K^*_M/K^*_{I_S}$ can be taken as the ratio of the relative interfacial affinities of the enzyme between the inhibitor and the substrate.

Table 4
Values of the ratio $K^*_M/K^*_I$ after curve fitting with Eq. (10) of the experimental data (Figs. 6 and 7) describing the lipase residual activity as a function of the inhibitor molar fraction of each enantiomer of compounds ($R_{11}Y_{16}$) and ($R_{16}Y_{11}$) on HPL, and ($R_{11}Y_{10}$) and ($R_{10}Y_{11}$) on HGL[a]

| | Ratio of $K^*_M/K^*_I$ | | | |
|---|---|---|---|---|
| | HGL | | HPL | |
| | Fast | Slow | Fast | Slow |
| ($R_{11}Y_{10}$) | 14 | 101 (86) | 22 | 102 |
| ($R_{10}Y_{11}$) | 12 | 133 (127) | 28 | 141 |
| ($R_{11}Y_{16}$) | 95 | 99 | 72 | 393 (386) |
| ($R_{16}Y_{11}$) | 26 | 17 | 22 | 277 (281) |

[a] Values in parenthesis indicate the ratio of $K^*_M/K^*_I$ based on the interfacial stoichiometry using Eq. (12).

## 4. Conclusion

The kinetic treatment of the experimentally data were analyzed using both the covalent and the pseudo-competitive inhibition models. For the first time, the relative interfacial affinity, $K^*_M/K^*_I$,

of HPL and HGL between each enantiomeric alkylphosphonate inhibitor and 1,2-dicaprin has been quantified.

From some of the experimental kinetic curves (Figs. 6 and 7), we can conclude that the observed inhibition can be correlated with a decrease in interfacial lipase binding to monomolecular films containing the enantiomeric inhibitors. In other words, the inhibition can be attributed to both interfacial binding as well as a chiral interaction of the inhibitor with the lipase active site. The chiral recognition of HPL and HGL may then occur not only at the active site but also during the initial adsorption step, assuming the interfacial lipase binding being controlled by a supramolecular chiral recognition process. However, up to now, the experimentally determined interfacial excess of lipase molecules includes all the enzymatic species, ($E^*$), ($E^*S$) and ($E^*I$). The proportions of each of these enzymatic species can not be experimentally determined. The present study supports the interfacial chiral recognition hypothesis in the case of mixed chiral films spread at a surface pressure of 20 mN $m^{-1}$, but further experiments are required to substantiate this theory.

## 5. Supplementary material

$^{31}P$, $^{1}H$, $^{13}C$ NMR, elemental analyses and $[\alpha]_D^{20}$ experimental data, HPLC separation methods of the phosphorus compounds **1**, **2**, and (RY). Data from the ELISA tests and details of covalent kinetic model are provided.

### *5.1. Experimental and physical data of organophosphorus compounds*

*5.1.1. Synthesis of alkylphosphonic acid dichloride 2-$R_{6-16}$ was performed as described for compound 2-$R_4$*

*5.1.1.1. n-Hexylphosphonic acid dichloride: 2-$R_6$.* Reflux 60 h. $Eb_{0.011} = 75°C$. Yield = 84%. $^{31}P$ NMR: $\delta$ 50.1; $^{1}H$ NMRNMR: $\delta$ 2.6 (m, 2H), 1.6 (m, 8H), 0.9 (t, 3H); $^{13}C$ NMR: $\delta$ 42.90 (d, P–$CH_2$, $^{1}J_{PC} = 96.1$ Hz), 30.98 (P–$(CH_2)_3$–$CH_2$), 29.15 (d, P–$CH_2$–$CH_2$–$CH_2$, $^{3}J_{PC} = 21.4$ Hz), 22.82 (d, P–$CH_2$–$CH_2$, $^{2}J_{PC} = 6.7$ Hz), 22.20 (P–$(CH_2)_4$–$CH_2$), 13.87 ($CH_3$).

*5.1.1.2. n-Octylphosphonic acid dichloride: 2-$R_8$.* Reflux 20 h. $Eb_{0.023} = 100°C$. Yield = 81%. $^{31}P$ NMR: $\delta$ 50.17; $^{1}H$ NMRNMR: $\delta$ 2.6 (m, 2H), 1.84 (m, 2H), 1.4 (m, 10H), 0.9 (t, 3H); $^{13}C$ NMR: $\delta$ 42.81 (d, P–$CH_2$, $^{1}J_{PC} = 96.5$ Hz), 31.49 (P–$(CH_2)_5$–$CH_2$), 29.38 (d, P–$CH_2$–$CH_2$–$CH_2$, $^{3}J_{PC} = 20.8$ Hz), 28.66 (P–$(CH_2)_3$–$(CH_2)_2$), 22.72 (d, P–$CH_2$–$CH_2$, $^{2}J_{PC} = 7.16$ Hz), 22.36 (P–$(CH_2)_6$–$CH_2$), 13.84 ($CH_3$).

*5.1.1.3. n-Decylphosphonic acid dichloride: 2-$R_{10}$.* Reflux 20 h. $Eb_{0.008} = 102°C$. Yield = 77%. $^{31}P$ NMR: $\delta$ 50.18; $^{1}H$ NMRNMR: $\delta$ 2.5 (m, 2H), 1.84 (m, 2H), 1.0–2.1 (m, 16H), 0.9 (t, 3H); $^{13}C$ NMR: $\delta$ 42.84 (d, P–$CH_2$, $^{1}J_{PC} = 96.3$ Hz), 33.22 (d, P–$CH_2$–$CH_2$–$CH_2$, $^{3}J_{PC} = 26.5$ Hz), 31.69 (P–$(CH_2)_7$–$CH_2$), 28.77 (P–$(CH_2)_3$–$CH_2$), 29.0–29.86 (P–$(CH_2)_4$–$(CH_2)_3$), 22.76 (d, P–$CH_2$–$CH_2$, $^{2}J_{PC} = 6.8$ Hz), 22.50 (P–$(CH_2)_8$–$CH_2$), 13.94 ($CH_3$).

*5.1.1.4. n-Undecyphosphonic acid dichloride: 2-$R_{11}$.* Reflux 72 h. $Eb_{0.008} = 170°C$. Yield = 95%. $^{31}P$ NMR: $\delta$ 50.30; $^{1}H$ NMRNMR: $\delta$ 2.4–2.8 (m, 2H), 0.8–2.1 (m, 21H); $^{13}C$ NMR: $\delta$ 43.0 (d, P–$CH_2$, $^{1}J_{PC} = 96.2$ Hz), 31.90 (P–$(CH_2)_8$–$CH_2$), 29.60 (d, P–$CH_2$–$CH_2$–$CH_2$, $^{3}J_{PC} = 21.5$ Hz), 29.30–29.50 (P–$(CH_2)_4$–$(CH_2)_4$), 28.91 (P–$(CH_2)_3$–$CH_2$), 22.89 (d, P–$CH_2$–$CH_2$, $^{2}J_{PC} = 6.9$ Hz), 22.67 (P–$(CH_2)_9$–$CH_2$), 14.10 ($CH_3$).

*5.1.1.5. n-Dodecyphosphonic acid dichloride: 2-$R_{12}$.* Reflux 20 h. $Eb_{0.003} = 120°C$. Yield = 82%. $^{31}P$ NMR: $\delta$ 50.27; $^{1}H$ NMRNMR: $\delta$ 2.5 (m, 2H), 1.0–2.1 (m, 20H), 0.9 (t, 3H); $^{13}C$ NMR: $\delta$ 42.92 (d, P–$CH_2$, $^{1}J_{PC} = 96.26$ Hz), 33.28 (d, P–$CH_2$–$CH_2$–$CH_2$, $^{3}J_{PC} = 26.6$ Hz),31.81 (P–$(CH_2)_9$–$CH_2$), 29.10–29.90 (P–$(CH_2)_4$–$(CH_2)_5$), 28.82 (P–$(CH_2)_3$–$CH_2$), 22.82 (d, P–$CH_2$–$CH_2$, $^{2}J_{PC} = 6.7$ Hz), 22.60 (P–$(CH_2)_{10}$–$CH_2$), 14.0 ($CH_3$).

*5.1.1.6. n-Tetradecyphosphonic acid dichloride: 2-$R_{14}$.* Reflux 20 h. $Eb_{0.008} = 130$°C. Yield = 57%. $^{31}$P NMR: $\delta$ 50.3; $^{1}$H NMRNMR: $\delta$ 2.55 (m, 2H), 1.0–2.1 (m, 24H), 0.9 (t, 3H); $^{13}$C NMR: $\delta$ 42.96 (d, P–*C*H$_2$, $^{1}J_{PC} = 96.3$ Hz), 33.31 (d, P–CH$_2$–CH$_2$–*C*H$_2$, $^{3}J_{PC} = 25.7$ Hz), 31.87 (P–(CH$_2$)$_{11}$–*C*H$_2$), 28.7–29.90 (P–(CH$_2$)$_3$–*(C*H$_2$)$_8$), 22.86 (d, P–CH$_2$–*C*H$_2$, $^{2}J_{PC} = 6.8$ Hz), 22.64 (P–(CH$_2$)$_{12}$–*C*H$_2$), 14.04 (*C*H$_3$).

*5.1.1.7. n-Hexadecyphosphonic acid dichloride: 2-$R_{16}$.* Reflux 20 h. $Eb_{0.008} = 150$°C. Yield = 57%. $^{31}$P NMR: $\delta$ 50.26; $^{1}$H NMRNMR: $\delta$ 2.6 (m, 2H), 1.0–2.1 (m, 28H), 0.9 (t, 3H); $^{13}$C NMR: $\delta$ 42.93 (d, P–*C*H$_2$, $^{1}J_{PC} = 96.3$ Hz), 33.07 (d, P–CH$_2$–CH$_2$–*C*H$_2$, $^{3}J_{PC} = 24.3$ Hz), 31.84 (P–(CH$_2$)$_{13}$–*C*H$_2$), 29.13–29.95 (P–(CH$_2$)$_3$–*(C*H$_2$)$_{10}$), 22.83 (d, P–CH$_2$–*C*H$_2$, $^{2}J_{PC} = 6.8$ Hz), 22.61 (P–(CH$_2$)$_{14}$–*C*H$_2$), 14.02 (*C*H$_3$).

*5.1.2. Synthesis of O-alkyl O-(p-nitrophenyl) n-undecylphosphoates ($R_{11}Y_{1-16}$) was performed as described for compound ($R_{11}Y_4$)*

*5.1.2.1. O-Methyl O-(p-nitrophenyl) n-undecylphosphonate: ($R_{11}Y_1$).* Flash chromatography: petroleum ether–ether 8:2 ($R_f = 0.48$, PMA). Yield 53%. $^{31}$P NMR: $\delta$ 30.9; $^{1}$H NMR: $\delta$ 8.3 (d, 2H$_{ar}$, $^{3}J = 9.0$ Hz), 7.4 (d, 2H$_{ar}$, $^{3}J = 9.0$ Hz), 3.8 (d, 3H, $^{3}J = 11.0$ Hz), 0.7–2.2 (m, 23H); $^{13}$C NMR: $\delta$ 155.77 (d, O–*C*$_{ar}$, $^{2}J_{PC} = 8.3$ Hz), 144.48 (*C*$_{ar}$–NO$_2$), 125.65 (O–C$_{ar}$–C$_{ar}$–*C*$_{ar}$), 120.90 (d, O–C$_{ar}$–*C*$_{ar}$, $^{3}J_{PC} = 4.8$ Hz), 53.04 (d, O–*C*H$_3$, $^{2}J_{PC} = 7.3$ Hz), 31.86 (P–(CH$_2$)$_8$–*C*H$_2$), 30.40 (d, P–CH$_2$–CH$_2$–*C*H$_2$, $^{3}J_{PC} = 17.4$ Hz), 29.29–29.53 (P–(CH$_2$)$_4$–*(C*H$_2$)$_4$), 28.98 (P–(CH$_2$)$_3$–*C*H$_2$), 25.52 (d, P–*C*H$_2$, $^{1}J_{PC} = 139.8$ Hz), 22.63 (P–(CH$_2$)$_9$–*C*H$_2$), 22.14 (d, P–CH$_2$–*C*H$_2$, $^{2}J_{PC} = 5.5$ Hz), 14.07 (P–(CH$_2$)$_{10}$–*C*H$_3$); Anal. Calc. for C$_{18}$H$_{30}$NO$_5$P (371.41): C 58.2, H 8.1, N 3.8, P 8.3%; found, C 59.7, H 8.8, N 3.4, P 8.6%.

*5.1.2.2. O-Hexyl O-(p-nitrophenyl) n-undecylphosphonate: ($R_{11}Y_6$).* Flash chromatography: petroleum ether–ether 7:3 ($R_f = 0.20$, PMA). Yield 53%. $^{31}$P NMR: $\delta$ 29.71; $^{1}$H NMR: $\delta$ 8.1 (d, 2H$_{ar}$, $^{3}J = 9.1$ Hz), 7.3 (d, 2H$_{ar}$, $^{3}J = 9.1$ Hz), 4.0 (m, 2H), 1.7 (m, 28H), 0.8 (t, 6H); $^{13}$C NMR: $\delta$ 155.45 (d, O–*C*$_{ar}$, $^{2}J_{PC} = 8.4$ Hz), 144.28 (*C*$_{ar}$–NO$_2$), 125.38 (O–C$_{ar}$–C$_{ar}$–*C*$_{ar}$), 120.79 (d, O–C$_{ar}$–*C*$_{ar}$, $^{3}J_{PC} = 4.5$ Hz), 66.84 (d, O–*C*H$_2$, $^{2}J_{PC} = 7.25$ Hz), 31.85 (P–(CH$_2$)$_8$–*C*H$_2$), 31.18 (O–(CH$_2$)$_3$–*C*H$_2$), 30.33 (d, P–CH$_2$–CH$_2$–*C*H$_2$, $^{3}J_{PC} = 16.9$ Hz), 30.31 (d, O–CH$_2$–*C*H$_2$, $^{3}J_{PC} = 5.6$ Hz), 29.28–29.52 (P–(CH$_2$)$_4$–*(C*H$_2$)$_4$, O–(CH$_2$)$_3$–*C*H$_2$), 28.98 (P–(CH$_2$)$_3$–*C*H$_2$), 25.72 (d, P–*C*H$_2$, $^{1}J_{PC} = 139.83$ Hz), 25.05 (O–CH$_2$–CH$_2$–*C*H$_2$), 22.45–22.63 (P–(CH$_2$)$_9$–*C*H$_2$, O–(CH$_2$)$_4$–*C*H$_2$), 22.14 (d, P–CH$_2$–*C*H$_2$, $^{2}J_{PC} = 5.4$ Hz), 14.03 (P–(CH$_2$)$_{10}$–*C*H$_3$); 13.86 (O–(CH$_2$)$_5$–*C*H$_3$); Anal. Calc. for C$_{23}$H$_{40}$NO$_5$P (441.54): C 62.6, H 9.1, N 3.2, P 7.0%; found, C 60.9, H 8.8, N 3.5, P 7.4%.

*5.1.2.3. O-Octyl O-(p-nitrophenyl) n-undecylphosphonate: ($R_{11}Y_8$).* Flash chromatography: petroleum ether–ether 7:3 ($R_f = 0.20$, PMA). Yield 36%. $^{31}$P NMR: $\delta$ 29.86; $^{1}$H NMR: $\delta$ 8.2 (d, 2H$_{ar}$, $^{3}J = 9.1$ Hz), 7.4 (d, 2H$_{ar}$, $^{3}J = 9.2$ Hz), 4.2 (m, 2H), 1.6 (m, 32H), 0.9 (t, 6H); $^{13}$C NMR: $\delta$ 155.54 (d, O–*C*$_{ar}$, $^{2}J_{PC} = 8.56$ Hz), 144.28 (*C*$_{ar}$–NO$_2$), 125.68 (O–C$_{ar}$–C$_{ar}$–*C*$_{ar}$), 120.02 (d, O–C$_{ar}$–*C*$_{ar}$, $^{3}J_{PC} = 4.6$ Hz), 67.24 (d, O–*C*H$_2$, $^{2}J_{PC} = 7.3$ Hz), 31.89 (P–(CH$_2$)$_8$–*C*H$_2$), 31.73 (O–(CH$_2$)$_5$–*C*H$_2$), 30.40 (d, P–CH$_2$–CH$_2$–*C*H$_2$, $^{3}J_{PC} = 16.9$ Hz), 30.38 (d, O–CH$_2$–*C*H$_2$, $^{3}J_{PC} = 6.1$ Hz), 29.02–29.57 (P–(CH$_2$)$_4$–*(C*H$_2$)$_4$, O–(CH$_2$)$_3$–*(C*H$_2$)$_2$), 29.14 (P–(CH$_2$)$_3$–*C*H$_2$), 25.74 (d, P–*C*H$_2$, $^{1}J_{PC} = 139.8$ Hz), 25.42 (O–CH$_2$–CH$_2$–*C*H$_2$), 22.67 (P–(CH$_2$)$_9$–*C*H$_2$, O–(CH$_2$)$_6$–*C*H$_2$), 22.16 (d, P–CH$_2$–*C*H$_2$, $^{2}J_{PC} = 5.67$ Hz), 14.06 (P–(CH$_2$)$_{10}$–*C*H$_3$, O–(CH$_2$)$_8$–*C*H$_3$); Anal. Calc. for C$_{25}$H$_{44}$NO$_5$P (469.60): C 63.9, H 9.4, N 3.0, P 6.6%; found, C 62.3, H 10.1, N 3.8, P 7.2%.

*5.1.2.4. O-Decyl O-(p-nitrophenyl) n-undecylphosphonate: ($R_{11}Y_{10}$).* Flash chromatography: petroleum ether–ether 7:3 ($R_f = 0.30$, PMA). Yield 60%. $^{31}$P NMR: $\delta$ 29.64; $^{1}$H NMR: $\delta$ 8.2 (d, 2H$_{ar}$, $^{3}J = 9.1$ Hz), 7.4 (d, 2H$_{ar}$, $^{3}J = 9.2$ Hz), 4.1 (m, 2H), 1.5–2.1 (m, 6H), 1.2 (m, 30H), 0.8 (t, 6H); $^{13}$C NMR: $\delta$ 155.72 (d, O–*C*$_{ar}$, $^{2}J_{PC} = 7.25$ Hz), 144.32 (*C*$_{ar}$–NO$_2$), 125.45 (O–C$_{ar}$–C$_{ar}$–*C*$_{ar}$), 120.83 (d, O–C$_{ar}$–*C*$_{ar}$, $^{3}J_{PC} = 4.25$ Hz), 66.75 (d, O–*C*H$_2$, $^{2}J_{PC} = 7.2$ Hz), 31.76 (P–(CH$_2$)$_8$–*C*H$_2$, O–(CH$_2$)$_7$–*C*H$_2$), 30.30 (d, O–CH$_2$–*C*H$_2$, $^{3}J_{PC} =$

6.39 Hz), 30.28 (d, P–$CH_2$–$CH_2$–$CH_2$, $^3J_{PC}$ = 16.97 Hz), 29.19–29.45 (P–$(CH_2)_4$–$(CH_2)_4$, O–$(CH_2)_3$–$(CH_2)_4$), 28.95 (P–$(CH_2)_3$–$CH_2$), 25.79 (d, P–$CH_2$, $^1J_{PC}$ = 139.35 Hz), 25.32 (O–$CH_2$–$CH_2$–$CH_2$), 22.54 (P–$(CH_2)_9$–$CH_2$, O–$(CH_2)_8$–$CH_2$), 22.11 (d, P–$CH_2$–$CH_2$, $^2J_{PC}$ = 5.66 Hz), 13.94 (P–$(CH_2)_{10}$–$CH_3$, O–$(CH_2)_9$–$CH_3$); Anal. Calc. for $C_{27}H_{48}NO_5P$ (497.65): C 65.2, H 9.7, N 2.8, P 6.2%; found, C 66.3, H 9.4, N 3.3, P 5.8%.

*5.1.2.5. O-Dodecyl O-(p-nitrophenyl) n-undecylphosphonate: ($R_{11}Y_{12}$).* Flash chromatography: petroleum ether–ether 7:3 ($R_f$ = 0.23, PMA). Yield 54%. $^{31}$P NMR: $\delta$ 29.45; $^1$H NMR: $\delta$ 8.2 (d, $2H_{ar}$, $^3J$ = 9.1 Hz), 7.4 (d, $2H_{ar}$, $^3J$ = 8.9 Hz), 4.0 (m, 2H), 1.8 (m, 4H), 1.2 (m, 36H), 0.7 (t, 6H); $^{13}$C NMR: $\delta$ 155.57 (d, O–$C_{ar}$, $^2J_{PC}$ = 8.3 Hz), 144.20 ($C_{ar}$–$NO_2$), 125.28 (O–$C_{ar}$–$C_{ar}$–$C_{ar}$), 120.69 (d, O–$C_{ar}$–$C_{ar}$, $^3J_{PC}$ = 5.0 Hz), 66.60 (d, O–$CH_2$, $^2J_{PC}$ = 7.2 Hz), 31.63 (P–$(CH_2)_8$–$CH_2$, O–$(CH_2)_9$–$CH_2$), 30.16 (d, O–$CH_2$–$CH_2$, $^3J_{PC}$ = 5.9 Hz), 30.13 (d, P–$CH_2$–$CH_2$–$CH_2$, $^3J_{PC}$ = 17.0 Hz), 29.06–29.30 (P–$(CH_2)_4$–$(CH_2)_4$, O–$(CH_2)_3$–$(CH_2)_6$), 28.79 (P–$(CH_2)_3$–$CH_2$), 25.64 (d, P–$CH_2$, $^1J_{PC}$ = 140.1 Hz), 25.17 (O–$CH_2$–$CH_2$–$CH_2$), 22.40 (P–$(CH_2)_9$–$CH_2$, O–$(CH_2)_{10}$–$CH_2$), 21.96 (d, P–$CH_2$–$CH_2$, $^2J_{PC}$ = 5.6 Hz), 13.79 (P–$(CH_2)_{10}$–$CH_3$, O–$(CH_2)_{11}$–$CH_3$); Anal. Calc. for $C_{29}H_{52}NO_5P$ (525.70): C 66.3, H 10.0, N 2.7, P 5.9%; found, C 67.9, H 11.3, N 3.1, P 6.1%.

*5.1.2.6. O-Tetradecyl O-(p-nitrophenyl) n-undecylphosphonate: ($R_{11}Y_{14}$).* Flash chromatography: petroleum ether–ether 7:3 ($R_f$ = 0.25, PMA). Yield 63%. $^{31}$P NMR: $\delta$ 29.49; $^1$H NMR: $\delta$ 8.1 (d, $2H_{ar}$, $^3J$ = 9.0 Hz), 7.3 (d, $2H_{ar}$, $^3J$ = 8.4 Hz), 4.0 (m, 2H), 1.9 (m, 1H), 1.6 (m, 4H), 1.2 (m, 39H), 0.8 (t, 6H); $^{13}$C NMR: $\delta$ 155.70 (d, O–$C_{ar}$, $^2J_{PC}$ = 8.6 Hz), 144.36 ($C_{ar}$–$NO_2$), 125.45 (O–$C_{ar}$–$C_{ar}$–$C_{ar}$), 120.84 (d, O–$C_{ar}$–$C_{ar}$, $^3J_{PC}$ = 4.4 Hz), 66.78 (d, O–$CH_2$, $^2J_{PC}$ = 7.2 Hz), 31.83 (P–$(CH_2)_8$–$CH_2$, O–$(CH_2)_{11}$–$CH_2$), 30.32 (d, O–$CH_2$–$CH_2$, $^3J_{PC}$ = 5.9 Hz), 30.29 (d, P–$CH_2$–$CH_2$–$CH_2$, $^3J_{PC}$ = 17.2 Hz), 29.23–29.56 (P–$(CH_2)_4$–$(CH_2)_4$, O–$(CH_2)_3$–$(CH_2)_8$), 28.96 (P–$(CH_2)_3$–$CH_2$), 25.80 (d, P–$CH_2$, $^1J_{PC}$ = 140.4 Hz), 25.32 (O–$CH_2$–$CH_2$–$CH_2$), 22.56 (P–$(CH_2)_9$–$CH_2$, O–$(CH_2)_{12}$–$CH_2$), 22.12 (d, P–$CH_2$–$CH_2$, $^2J_{PC}$ = 5.7 Hz), 13.95 (P–$(CH_2)_{10}$–$CH_3$, O–$(CH_2)_{13}$–$CH_3$); Anal. Calc. for $C_{31}H_{56}NO_5P$ (553.76): C 67.2, H 10.2, N 2.5, P 5.6%; found, C 66.5, H 11.1, N 2.9, P 6.0%.

*5.1.2.7. O-Hexadecyl O-(p-nitrophenyl) n-undecylphosphonate: ($R_{11}Y_{16}$).* Flash chromatography: petroleum ether–ether 7:3 ($R_f$ = 0.27, PMA). Yield 66%. $^{31}$P NMR: $\delta$ 29.28; $^1$H NMR: $\delta$ 8.2 (d, $2H_{ar}$, $^3J$ = 7.8 Hz), 7.4 (d, $2H_{ar}$, $^3J$ = 9.2 Hz), 4.1 (m, 2H), 1.9 (m, 1H), 1.7 (m, 3H), 1.2 (m, 44H), 0.8 (t, 6H); $^{13}$C NMR: $\delta$ 155.63 (d, O–$C_{ar}$, $^2J_{PC}$ = 8.6 Hz), 144.29 ($C_{ar}$–$NO_2$), 125.39 (O–$C_{ar}$–$C_{ar}$–$C_{ar}$), 120.77 (d, O–$C_{ar}$–$C_{ar}$, $^3J_{PC}$ = 4.5 Hz), 66.71 (d, O–$CH_2$, $^2J_{PC}$ = 7.2 Hz), 31.81 (P–$(CH_2)_8$–$CH_2$, O–$(CH_2)_{13}$–$CH_2$), 30.32 (d, O–$CH_2$–$CH_2$, $^3J_{PC}$ = 6.0 Hz), 30.31 (d, P–$CH_2$–$CH_2$–$CH_2$, $^3J_{PC}$ = 16.2 Hz), 29.23–29.60 (P–$(CH_2)_4$–$(CH_2)_4$, O–$(CH_2)_3$–$(CH_2)_{10}$), 28.98 (P–$(CH_2)_3$–$CH_2$), 25.82 (d, P–$CH_2$, $^1J_{PC}$ = 139.66 Hz), 25.35 (O–$CH_2$–$CH_2$–$CH_2$), 22.58 (P–$(CH_2)_9$–$CH_2$, O–$(CH_2)_{14}$–$CH_2$), 22.12 (d, P–$CH_2$–$CH_2$, $^2J_{PC}$ = 5.7 Hz), 13.98 (P–$(CH_2)_{10}$–$CH_3$, O–$(CH_2)_{15}$–$CH_3$); Anal. Calc. for $C_{33}H_{60}NO_5P$ (581.81): C 68.1, H 10.4, N 2.4, P 5.3%; found, C 69.2, H 10.7, N 2.9, P 6.0%.

*5.1.3. Synthesis of O-(n-undecyl) O-(p-nitrophenyl) alkylphosphoates ($R_{1-16}Y_{11}$) was performed as described for compound ($R_1Y_{11}$)*

*5.1.3.1. O-(n-Undecyl) O-(p-nitrophenyl) butylphosphonate: ($R_4Y_{11}$).* Flash chromatography: petroleum ether–ether 7:3 ($R_f$ = 0.25, PMA). Yield 66%. $^{31}$P NMR: $\delta$ 29.62; $^1$H NMR: $\delta$ 8.2 (d, $2H_{ar}$, $^3J$ = 9.07 Hz), 7.4 (d, $2H_{ar}$, $^3J$ = 10.27 Hz), 4.2 (m, 2H), 1.1–2.2 (m, 24H), 0.9 (t, 6H); $^{13}$C NMR: $\delta$ 155.61 (d, O–$C_{ar}$, $^2J_{PC}$ = 8.16 Hz), 144.21 ($C_{ar}$–$NO_2$), 125.40 (O–$C_{ar}$–$C_{ar}$–$C_{ar}$), 120.74 (d, O–$C_{ar}$–$C_{ar}$, $^3J_{PC}$ = 4.8 Hz), 66.66 (d, O–$CH_2$, $^2J_{PC}$ = 7.3 Hz), 31.67 (O–$(CH_2)_8$–$CH_2$), 30.18 (d, O–$CH_2$–$CH_2$, $^3J_{PC}$ = 5.87 Hz), 29.10–29.30 (O–$(CH_2)_4$–$(CH_2)_4$), 28.83 (O–$(CH_2)_3$–$CH_2$), 25.41 (d, P–$CH_2$, $^1J_{PC}$ = 140.4 Hz), 25.18 (O–$CH_2$–$CH_2$–$CH_2$), 24.04 (d, P–$CH_2$–$CH_2$, $^2J_{PC}$ = 5.6 Hz), 22.45 (O–$(CH_2)_9$–$CH_2$), 23.94 (d,

P–$CH_2$–$CH_2$–$CH_2$, $^3J_{PC}$ = 17.8 Hz), 13.86 (O–$(CH_2)_{10}$–$CH_3$), 13.29 (P–$(CH_2)_3$–$CH_3$); Anal. Calc. for $C_{21}H_{36}NO_5P$ (413.49): C 61.0, H 8.8, N 3.4, P 7.5%; found, C 62.1, H 9.6, N 3.7, P 8.1%.

*5.1.3.2. O-(n-Undecyl) O-(p-nitrophenyl) hexylphosphonate: ($R_6Y_{11}$).* Flash chromatography: petroleum ether–ether 7:3 ($R_f$ = 0.25, PMA). Yield 67%. $^{31}$P NMR: $\delta$ 29.54; $^1$H NMR: $\delta$ 8.2 (d, 2$H_{ar}$, $^3J$ = 9.2 Hz), 7.4 (d, 2$H_{ar}$, $^3J$ = 10.02 Hz), 4.2 (m, 2H), 1.1–2.2 (m, 28H), 0.9 (t, 6H); $^{13}$C NMR: $\delta$ 155.60 (d, O–$C_{ar}$, $^2J_{PC}$ = 8.4 Hz), 144.18 ($C_{ar}$–$NO_2$), 125.34 (O–$C_{ar}$–$C_{ar}$–$C_{ar}$), 120.72 (d, O–$C_{ar}$–$C_{ar}$, $^3J_{PC}$ = 4.53 Hz), 66.63 (d, O–$CH_2$, $^2J_{PC}$ = 7.27 Hz), 31.66 (O–$(CH_2)_8$–$CH_2$), 30.95 (P–$(CH_2)_3$–$CH_2$), 30.18 (d, O–$CH_2$–$CH_2$, $^3J_{PC}$ = 5.9 Hz), 29.85 (d, P–$CH_2$–$CH_2$–$CH_2$, $^3J_{PC}$ = 17.05 Hz), 28.83–29.30 (O–$(CH_2)_3$–$(CH_2)_5$), 25.67 (d, P–$CH_2$, $^1J_{PC}$ = 140.2 Hz), 25.19 (O–$CH_2$–$CH_2$–$CH_2$), 22.44 (P–$(CH_2)_4$–$CH_2$, O–$(CH_2)_9$–$CH_2$), 22.0 (d, P–$CH_2$–$CH_2$, $^2J_{PC}$ = 6.8 Hz), 13.78 (P–$(CH_2)_5$–$CH_3$, O–$(CH_2)_{10}$–$CH_3$); Anal. Calc. for $C_{23}H_{40}NO_5P$ (441.54): C 62.6, H 9.1, N 3.2, P 7.0%; found, C 61.2, H 9.5, N 2.9, P 6.5%.

*5.1.3.3. O-(n-Undecyl) O-(p-nitrophenyl) octylphosphonate: ($R_8Y_{11}$).* Flash chromatography: petroleum ether–ether 7:3 ($R_f$ = 0.25, PMA). Yield 79%. $^{31}$P NMR: $\delta$ 29.5; $^1$H NMR: $\delta$ 8.2 (d, 2$H_{ar}$, $^3J$ = 9.16 Hz), 7.4 (d, 2$H_{ar}$, $^3J$ = 10.16 Hz), 4.2 (m, 2H), 1.1–2.2 (m, 32H), 0.9 (t, 6H); $^{13}$C NMR: $\delta$ 155.84 (d, O–$C_{ar}$, $^2J_{PC}$ = 8.6 Hz), 144.41 ($C_{ar}$–$NO_2$), 125.56 (O–$C_{ar}$–$C_{ar}$–$C_{ar}$), 120.93 (d, O–$C_{ar}$–$C_{ar}$, $^3J_{PC}$ = 4.66 Hz), 66.82 (d, O–$CH_2$, $^2J_{PC}$ = 7.33 Hz), 31.82 (P–$(CH_2)_5$–$CH_2$, O–$(CH_2)_8$–$CH_2$), 30.41 (d, P–$CH_2$–$CH_2$–$CH_2$, $^3J_{PC}$ = 16.85 Hz), 30.40 (d, O–$CH_2$–$CH_2$, $^3J_{PC}$ = 6.1 Hz), 28.90–29.50 (P–$(CH_2)_3$–$(CH_2)_3$, O–$(CH_2)_3$–$(CH_2)_5$), 25.91 (d, P–$CH_2$, $^1J_{PC}$ = 140.0 Hz), 25.55 (O–$CH_2$–$CH_2$–$CH_2$), 22.60 (P–$(CH_2)_6$–$CH_2$, O–$(CH_2)_9$–$CH_2$), 22.22 (d, P–$CH_2$–$CH_2$, $^2J_{PC}$ = 5.64 Hz), 14.04 (P–$(CH_2)_7$–$CH_3$, O–$(CH_2)_{10}$–$CH_3$); Anal. Calc. for $C_{25}H_{44}NO_5P$ (469.60): C 63.9, H 9.4, N 3.0, P 6.6%; found, C 64.3, H 9.9, N 3.7, P 5.8%.

*5.1.3.4. O-(n-Undecyl) O-(p-nitrophenyl) decylphosphonate: ($R_{10}Y_{11}$).* Flash chromatography: petroleum ether–ether 7:3 ($R_f$ = 0.25, PMA). Yield 71%. $^{31}$P NMR: $\delta$ 29.55; $^1$H NMR: $\delta$ 8.2 (d, 2$H_{ar}$, $^3J$ = 9.2 Hz), 7.4 (d, 2$H_{ar}$, $^3J$ = 9.95 Hz), 4.2 (m, 2H), 1.0–2.1 (m, 36H), 0.9 (t, 6H); $^{13}$C NMR: $\delta$ 155.80 (d, O–$C_{ar}$, $^2J_{PC}$ = 8.26 Hz), 144.40 ($C_{ar}$–$NO_2$), 125.55 (O–$C_{ar}$–$C_{ar}$–$C_{ar}$), 120.92 (d, O–$C_{ar}$–$C_{ar}$, $^3J_{PC}$ = 4.8 Hz), 66.81 (d, O–$CH_2$, $^2J_{PC}$ = 7.27 Hz), 31.88 (P–$(CH_2)_7$–$CH_2$, O–$(CH_2)_8$–$CH_2$), 30.41 (d, O–$CH_2$–$CH_2$, $^3J_{PC}$ = 6.1 Hz), 30.40 (d, P–$CH_2$–$CH_2$–$CH_2$, $^3J_{PC}$ = 16.77 Hz), 28.30–29.50 (P–$(CH_2)_4$–$(CH_2)_3$, O–$(CH_2)_3$–$(CH_2)_5$), 28.69 (P–$(CH_2)_3$–$CH_2$), 25.91 (d, P–$CH_2$, $^1J_{PC}$ = 140.0 Hz), 25.42 (O–$CH_2$–$CH_2$–$CH_2$), 22.86 (P–$(CH_2)_8$–$CH_2$, O–$(CH_2)_9$–$CH_2$), 22.22 (d, P–$CH_2$–$CH_2$, $^2J_{PC}$ = 5.46 Hz), 14.06 (P–$(CH_2)_9$–$CH_3$, O–$(CH_2)_{10}$–$CH_3$); Anal. Calc. for $C_{27}H_{48}NO_5P$ (497.65): C 65.2, H 9.7, N 2.8, P 6.2%; found, C 64.8, H 10.5, N 3.6, P 7.1%.

*5.1.3.5. O-(n-Undecyl) O-(p-nitrophenyl) dodecylphosphonate: ($R_{12}Y_{11}$).* Flash chromatography: petroleum ether–ether 7:3 ($R_f$ = 0.25, PMA). Yield 70%. $^{31}$P NMR: $\delta$ 29.60; $^1$H NMR: $\delta$ 8.23 (d, 2$H_{ar}$, $^3J$ = 9.2 Hz), 7.4 (d, 2$H_{ar}$, $^3J$ = 9.98 Hz), 4.14 (m, 2H), 1.1–2.2 (m, 40H), 0.9 (t, 6H); $^{13}$C NMR: $\delta$ 155.56 (d, O–$C_{ar}$, $^2J_{PC}$ = 8.16 Hz), 144.30 ($C_{ar}$–$NO_2$), 125.40 (O–$C_{ar}$–$C_{ar}$–$C_{ar}$), 120.80 (d, O–$C_{ar}$–$C_{ar}$, $^3J_{PC}$ = 4.6 Hz), 66.77 (d, O–$CH_2$, $^2J_{PC}$ = 7.33 Hz), 31.75 (P–$(CH_2)_9$–$CH_2$, O–$(CH_2)_8$–$CH_2$), 30.25 (d, O–$CH_2$–$CH_2$, $^3J_{PC}$ = 5.97 Hz), 30.23 (d, P–$CH_2$–$CH_2$–$CH_2$, $^3J_{PC}$ = 16.92 Hz), 28.90–29.44 (P–$(CH_2)_3$–$(CH_2)_6$, O–$(CH_2)_3$–$(CH_2)_5$), 25.68 (d, P–$CH_2$, $^1J_{PC}$ = 139.88 Hz), 25.27 (O–$CH_2$–$CH_2$–$CH_2$), 22.52 (P–$(CH_2)_{10}$–$CH_2$, O–$(CH_2)_9$–$CH_2$), 22.05 (d, P–$CH_2$–$CH_2$, $^2J_{PC}$ = 5.62 Hz), 13.91 (P–$(CH_2)_{11}$–$CH_3$, O–$(CH_2)_{10}$–$CH_3$); Anal. Calc. for $C_{29}H_{52}NO_5P$ (525.70): C 66.3, H 10.0, N 2.7, P 5.9%; found, C 67.1, H 9.5, N 3.1, P 5.4%.

*5.1.3.6. O-(n-Undecyl) O-(p-nitrophenyl) tetradecylphosphonate: ($R_{14}Y_{11}$).* Flash chromatography: petroleum ether–ether 7:3 ($R_f$ = 0.25, PMA). Yield 40%. $^{31}$P NMR: $\delta$ 29.68; $^1$H NMR: $\delta$ 8.24 (d, 2$H_{ar}$, $^3J$ = 8.9 Hz), 7.4 (d, 2$H_{ar}$, $^3J$ = 9.27 Hz),

Table 5
Eluent of separation, retention time ($t_R$) and rotatory power of each enantiomer of compounds ($R_{11}Y_{1-16}$)

| ($R_{11}Y_{1-16}$) | | Eluent:hexane–2-propanol | $t_R$ (min) | | $[\alpha]_D^{20}$ |
|---|---|---|---|---|---|
| 1 | $CH_3$ | 90:10 | 8.50 | +9.0 | (*c* 0.2, $CH_2Cl_2$) |
| | | | 12.80 | −9.0 | |
| 4 | $C_4H_9$ | 98:2 | 14.04 | +2.37 | (*c* 3.63, $CH_2Cl_2$) |
| | | | 17.52 | −2.37 | |
| 6 | $C_6H_{11}$ | 95:5 | 10.26 | +0.93 | (*c* 3.34, $CH_2Cl_2$) |
| | | | 16.34 | −0.93 | |
| 8 | $C_8H_{17}$ | 99:1 | 21.70 | +0.44 | (*c* 3.66, $CH_2Cl_2$) |
| | | | 28.90 | −0.44 | |
| 10 | $C_{10}H_{21}$ | 99.5:0.5 | 14.74 | −2.25 | (*c* 1.56, $CH_2Cl_2$) |
| | | | 19.55 | 2.25 | |
| 12 | $C_{12}H_{25}$ | 99.5:0.5 | 20.41 | −0.85 | (*c* 1.53, $CH_2Cl_2$) |
| | | | 25.34 | 0.85 | |
| 14 | $C_{14}H_{29}$ | 99.5:0.5 | 17.01 | −0.47 | (*c* 2.8, $CH_2Cl_2$) |
| | | | 20.70 | 0.47 | |
| 16 | $C_{16}H_{33}$ | 99.5:0.5 | 14.36 | −0.52 | (*c* 5.56, $CH_2Cl_2$) |
| | | | 16.98 | 0.52 | |

4.12 (m, 2H), 1.0–2.2 (m, 47H), 0.9 (t, 6H); $^{13}$C NMR: $\delta$ 155.54 (d, O–$C_{ar}$, $^2J_{PC} = 8.32$ Hz), 144.32 ($C_{ar}$–$NO_2$), 125.59 (O–$C_{ar}$–$C_{ar}$–$C_{ar}$), 120.89 (d, O–$C_{ar}$–$C_{ar}$, $^3J_{PC} = 4.83$ Hz), 66.93 (d, O–$CH_2$, $^2J_{PC} = 7.1$ Hz), 31.85 (P–$(CH_2)_{11}$–$CH_2$, O–$(CH_2)_8$–$CH_2$), 30.36 (d, O–$CH_2$–$CH_2$, $^3J_{PC} =$ 6.13 Hz), 30.35 (d, P–$CH_2$–$CH_2$–$CH_2$, $^3J_{PC} =$ 16.34 Hz), 29.0–29.50 (P–$(CH_2)_3$–$(CH_2)_8$, O–$(CH_2)_3$–$(CH_2)_5$), 25.84 (d, P–$CH_2$, $^1J_{PC} =$ 139.92 Hz), 25.40 (O–$CH_2$–$CH_2$–$CH_2$), 22.37 (P–$(CH_2)_{12}$–$CH_2$, O–$(CH_2)_9$–$CH_2$), 22.12 (d, P–$CH_2$–$CH_2$, $^2J_{PC} = 5.0$ Hz), 14.04 (P–$(CH_2)_{13}$–$CH_3$, O–$(CH_2)_{10}$–$CH_3$); Anal. Calc. for $C_{31}H_{56}NO_5P$ (553.76): C 67.2, H 10.2, N 2.5, P 5.6%; found, C 68.5, H 9.6, N 2.1, P 6.3%.

*5.1.3.7. O-(n-Undecyl) O-(p-nitrophenyl) hexadecylphosphonate: ($R_{16}Y_{11}$).* Flash chromatography: petroleum ether–ether 7:3 ($R_f = 0.25$, PMA). Yield 60%. $^{31}$P NMR: $\delta$ 29.71; $^1$H NMR: $\delta$ 8.23 (d, $2H_{ar}$, $^3J = 9.14$ Hz), 7.4 (d, $2H_{ar}$, $^3J = 9.19$ Hz), 4.13 (m, 2H), 1.0–2.1 (m, 48H), 0.9 (t, 6H); $^{13}$C NMR: $\delta$ 155.52 (d, O–$C_{ar}$, $^2J_{PC} = 8.48$ Hz), 144.39 ($C_{ar}$–$NO_2$), 125.49 (O–$C_{ar}$–$C_{ar}$–$C_{ar}$), 120.83 (d, O–$C_{ar}$–$C_{ar}$, $^3J_{PC} = 4.7$ Hz), 66.90 (d, O–$CH_2$, $^2J_{PC} = 7.33$ Hz), 31.79 (P–$(CH_2)_{13}$–$CH_2$, O–$(CH_2)_8$–$CH_2$), 30.27 (d, P–$CH_2$–$CH_2$–$CH_2$, $^3J_{PC} = 16.9$ Hz), 30.26 (d, O–$CH_2$–$CH_2$, $^3J_{PC} =$ 5.95 Hz), 28.90–29.60 (P–$(CH_2)_3$–$(CH_2)_{11}$, O–$(CH_2)_3$–$(CH_2)_5$), 25.70 (d, P–$CH_2$, $^1J_{PC} = 140.29$ Hz), 25.30 (O–$CH_2$–$CH_2$–$CH_2$), 22.56 (P–$(CH_2)_{14}$–$CH_2$, O–$(CH_2)_9$–$CH_2$), 22.06 (d, P–$CH_2$–$CH_2$, $^2J_{PC} = 5.62$ Hz), 13.96 (P–$(CH_2)_{15}$–$CH_3$, O–$(CH_2)_{10}$–$CH_3$); Anal. Calc. for $C_{33}H_{60}NO_5P$ (581.81): C 68.1, H 10.4, N 2.4, P 5.3%; found, C 67.5, H 11.8, N 3.1, P 5.9%.

The separation of each enantiomer alkylphosphonate was performed on a Water HPLC system using a Daicel Chiralpack AS column 250 × 250 mm, and a Waters UV detector at $\lambda = 254$ nm. The HPLC analysis were carried out at 25°C using *n*-hexane–2-propanol as eluent; flow rate 4.5 ml min$^{-1}$. Ten injections of 100 μl (100 mg ml$^{-1}$) sample phosphonates gave each enantiomer in 99% *ee*. Tables 5 and 6 gave the different proportions of *n*-hexane and 2-propanol used in the HPLC separation, the retention time and the rotatory powers of each enantiomer of alkylphosphonates (RY).

## 5.2. Covalent kinetic model

### 5.2.1. Theoretical expressions

Sigmoidal expression of the time dependence of product released:

$$P = k_{cat} \cdot E_0 \cdot \frac{S}{K^*_M} \cdot \frac{1}{I_R \cdot \frac{k_{i_R}}{K^*_{I_R}} + I_S \cdot \frac{k_{i_S}}{K^*_{I_S}}} \cdot \frac{\tau_1 \cdot (1 - e^{-t/\tau_1}) - \tau_2 \cdot (1 - e^{-t/\tau_2})}{\tau_1 - \tau_2}$$

The corresponding equation of the enzymatic velocity is:

$$v = \frac{dP}{dt} = k_{cat} \cdot E_0 \cdot \frac{S}{K^*_M} \cdot \frac{1}{I_R \cdot \frac{k_{i_R}}{K^*_{I_R}} + I_S \cdot \frac{K_{i_S}}{K^*_{I_S}}} \cdot \frac{e^{-t/\tau_1} - e^{-t/\tau_2}}{\tau_1 - \tau_2}$$

with

$$\tau_1 = \frac{\frac{2}{k_d} \cdot \left(1 + \frac{S}{K^*_M} + \frac{I}{K^*_I}\right)}{X - \sqrt{X^2 - 4 \cdot \frac{k_i}{k_d} \cdot \frac{I}{K^*_I} \cdot \frac{k_p \cdot {}^A/_V}{k_d} \cdot \left(1 + \frac{S}{K^*_M} + \frac{I}{K^*_I}\right)}}$$

$$\tau_2 = \frac{\frac{2}{k_d} \cdot \left(1 + \frac{S}{K^*_M} + \frac{I}{K^*_I}\right)}{X + \sqrt{X^2 - 4 \cdot \frac{k_i}{k_d} \cdot \frac{I}{K^*_I} \cdot \frac{k_p \cdot {}^A/_V}{k_d} \cdot \left(1 + \frac{S}{K^*_M} + \frac{I}{K^*_I}\right)}}$$

and

$$X = 1 + \frac{k_p \cdot {}^A/_V}{k_d} \cdot \left(1 + \frac{S}{K^*_M} + \frac{I}{K^*_I}\right) + \frac{k_i}{k_d} \cdot \frac{I}{K^*_I}$$

$$K^*_M = \frac{k_{-1} + k_{cat}}{k_1}$$

*5.2.2. Recalculation, in the case of compounds ($R_{11}Y_{16}$) and ($R_{16}Y_{11}$), of the $\alpha_{50}$ values from Ks, Kf, $\tau_1$ and $\tau_2$ theoretical data*

Ransac et al. (1990, 1991) defined a velocities ratio as: $R_v$ = (velocity in the presence of an inhibitor with $K^*_I = K^*_M$)/(velocity in the presence of an inhibitor with $K^*_I \neq K^*_M$).

This ratio varies linearly with the inhibitor molar fraction ($\alpha$) and can be rewritten as:

$$R_v = (1 - \alpha) \cdot \left(\frac{V_{1,2-dicaprin}}{V_{inflexion}}\right) = 1 + \alpha \cdot Z$$

where $v_{1,2\text{-dicaprin}}$ is the maximal value of the enzyme velocity in the presence of a film of 1,2-dicaprin; and $v_{inflexion}$ is the maximal value of the enzyme velocity in the presence of a mixed film of inhibitor–1,2-dicaprin.

The molar fraction of inhibitor which reduces the enzyme activity to 50% of its initial value, $\alpha_{50}$, can then be written as:

$$\alpha_{50} = \frac{1}{2 + Z}$$

Table 6
Eluent of separation, retention time ($t_R$) and rotatory power of each enantiomer of compounds ($R_{1-16}Y_{11}$)

| ($R_{1-16}Y_{11}$) | | Eluent:hexane–2-propanol | $t_R$ | $[\alpha]^{20}_D$ | |
|---|---|---|---|---|---|
| 1 | $CH_3$ | 99.5:0.5 (not separated) | 42.59 | | – |
| 4 | $C_4H_9$ | 99.5:0.5 (not separated) | 48.04 | | – |
| 6 | $C_6H_{11}$ | 99.5:0.5 | 30.82 | −1.16 | (*c* 4.32, $CH_2Cl_2$) |
| | | | 36.29 | +1.16 | |
| 8 | $C_8H_{17}$ | 99:1 | 25.90 | −0.96 | (*c* 3.43, $CH_2Cl_2$) |
| | | | 30.86 | +0.96 | |
| 10 | $C_{10}H_{21}$ | 99.5:0.5 | 21.19 | −0.62 | (*c* 4.53, $CH_2Cl_2$) |
| | | | 24.08 | +0.62 | |
| 12 | $C_{12}H_{25}$ | 99.5:0.5 | 19.29 | −0.48 | (*c* 4.78, $CH_2Cl_2$) |
| | | | 24.06 | +0.48 | |
| 14 | $C_{14}H_{29}$ | 99.5:0.5 | 16.14 | −0.39 | (*c* 3.82, $CH_2Cl_2$) |
| | | | 19.95 | +0.39 | |
| 16 | $C_{16}H_{33}$ | 99.5:0.5 | 13.27 | −0.27 | (*c* 5.56, $CH_2Cl_2$) |
| | | | 15.98 | +0.27 | |

Table 7
HPL superficial concentration, $\Gamma$ (pg cm$^{-2}$), determined by an ELISA with monomolecular films of mixed inhibitor ($R_{16}Y_{11}$)–1,2-dicaprin at $\pi = 20$ mN m$^{-1}$ after 15 min of incubation[a]

| Films | (%) | HPL concentration in recovered film (ng ml$^{-1}$) | HPL concentration in bulk phase (ng ml$^{-1}$) | Total recovery (%) | HPL superficial concentration $\Gamma$ (pg cm$^{-2}$) | Film adsorbed lipase (%) |
|---|---|---|---|---|---|---|
| 1,2-dicaprin | | 24.7/23.8 | 10.2/10.3 | 54/52 | 224.6/207.0 | 0.69/0.65 |
| *Fast* | 100 | 19.3/19.1 | 19.5/19.3 | 97/96 | 0.0/0.0 | 0.0/0.0 |
| | 60 | 19.2/18.4 | 19.6/18.7 | 98/93 | 0.0/0.0 | 0.0/0.0 |
| | 30 | 20.5/16.0 | 20.9/16.3 | 100/84 | 0.0/0.0 | 0.0/0.0 |
| | 15 | 16.0/14.9 | 9.7/12.0 | 50/62 | 83.0/79.2 | 0.26/0.25 |
| | 10 | 15.9/16.7 | 12.4/10.1 | 64/52 | 96.9/88.0 | 0.30/0.27 |
| | 5 | 19.3/21.6 | 14.7/16.4 | 74/85 | 115.5/136.1 | 0.36/0.42 |
| *Slow* | 100 | 14.4/16.0 | 14.6/16.2 | 73/81 | 0.0/0.0 | 0.0/0.0 |
| | 60 | 15.5/17.8 | 15.8/18.1 | 80/90 | 0.0/0.0 | 0.0/0.0 |
| | 30 | 14.0/13.4 | 12.6/9.1 | 65/46 | 42.7/67.8 | 0.13/0.21 |
| | 15 | 17.2/15.3 | 14.4/12.4 | 74/64 | 79.3/86.2 | 0.25/0.27 |
| | 10 | 18.7/17.4 | 12.0/10.6 | 62/55 | 119.5/122.7 | 0.37/0.38 |
| | 5 | 17.0/18.8 | 10.9/12.6 | 55/66 | 197.5/200.0 | 0.61/0.62 |

[a] We have, however, measured the interfacial binding of HPL on pure films of ($R_{16}Y_{11}$)s and ($R_{16}Y_{11}$)f as a function of surface pressure. At 15 and 20 mN m$^{-1}$ no significant surface excess of HPL could be detected. In contrast, at 10 mN m$^{-1}$ a substantial interfacial binding was measured: 41.6 and 107.1 pg cm$^{-2}$ of HPL in the case of ($R_{16}Y_{11}$)s and ($R_{16}Y_{11}$)f, respectively. Furthermore, this surface excess values increase by about 1.7-fold when working on pure films of the same phosphonate compounds spread at 5 mN m$^{-1}$ (data not shown).

Table 8
HGL superficial concentration, $\Gamma$ (pg cm$^{-2}$), determined by an ELISA with monomolecular films of mixed inhibitor ($R_{10}Y_{11}$)–1,2-dicaprin at $\pi = 20$ mN m$^{-1}$ after 15 min incubation

| Films | (%) | HGL concentration in recovered film (ng ml$^{-1}$) | HGL concentration in bulk phase (ng ml$^{-1}$) | Total recovery (%) | HGL superficial concentration $\Gamma$ (pg cm$^{-2}$) | Film adsorbed lipase (%) |
|---|---|---|---|---|---|---|
| 1,2-dicaprin | | 206.8/210.5 | 183.2/181.7 | 64/63 | 911.8/1111.9 | 0.193/0.236 |
| *Fast* | 100 | 206.9/201.6 | 198.1/192.8 | 69/67 | 146.9/147.5 | 0.03/0.03 |
| | 60 | 239.7/237.4 | 232.3/230.9 | 81/80 | 187.8/167.0 | 0.04/0.03 |
| | 30 | 240.6/238.3 | 232.8/230.6 | 81/80 | 211.0/210.0 | 0.05/0.04 |
| | 15 | 221.0/216.4 | 204.6/199.3 | 71/69 | 301.8/313.1 | 0.06/0.07 |
| | 10 | 222.8/223.6 | 212.5/213.3 | 74/74 | 359.1/356.4 | 0.08/0.08 |
| | 5 | 227.2/229.3 | 210.7/214.0 | 73/74 | 485.1/452.5 | 0.10/0.10 |
| *Slow* | 100 | 227.2/232.2 | 210.7/212.8 | 73/74 | 378.1/422.7 | 0.08/0.09 |
| | 60 | 207.2/215.7 | 184.1/188.9 | 64/66 | 424.9/493.7 | 0.09/0.10 |
| | 30 | 272.4/274.3 | 253.5/260.5 | 90/91 | 568.7/565.8 | 0.12/0.12 |

Example: in the case of compound ($R_{16}Y_{11}$)

$V_{1,2\text{-dicaprin}} = 8.78 \text{ mm min}^{-1}$

From Eq. (4) and data presented in Table 3, we obtain, at $ee = -50\%$.

| Inhibitor molar fraction ($\alpha$) | $v_{\text{inflexion}}$ | $R_v$ |
|---|---|---|
| 0.00 | $V_{1,2\text{-dicaprin}}$ | 1.00 |
| 0.01 | 3.23 | 2.70 |
| 0.03 | 2.12 | 4.02 |
| 0.05 | 1.20 | 6.95 |
| 0.07 | 0.65 | 12.56 |

By linear regression of $R_v = f(\alpha)$, we deduced the following $\alpha_{50}$ value:

$$R_v = 1 + 153.3\ \alpha \quad \Rightarrow \alpha_{50} = \frac{1}{2 + 153.3} \cdot 100 = 0.64\%$$

### 5.3. ELISA tests for measuring the HPL and HGL interfacial binding

HPL (19.4 ng ml$^{-1}$, final concentration in the sub-phase) at pH 8 (Table 7), and HGL (288.4 ng ml$^{-1}$, final concentration in the sub-phase) at pH 5 (Table 8), were recovered after 15 min incubation to monomolecular films (20 mN m$^{-1}$) of 1,2-dicaprin mixed with different molar fraction of inhibitor ($R_{16}Y_{11}$) for HPL as depicted in Fig. 6; and inhibitor ($R_{10}Y_{11}$) for HGL as depicted in Fig. 7.

Each experiment was performed in duplicate (see Section 2 for details).

## Acknowledgements

We thank the Conseil Régional de la Région PACA for a PhD financial support. This research was carried out under the BIOTECH G-Lipase (contract BIO2-CT94-3041) Program of the European Union.

## References

Andelman, D., 1989. Chiral discrimination and phase transitions in Langmuir monolayers. J. Am. Chem. Soc. 111, 6536–6544.

Aoubala, M., Daniel, C., De Caro, A., Ivanova, M.G., Hirn, M., Sarda, L., Verger, R., 1993. Epitope mapping and immunoactivation of human gastric lipase using five monoclonal antibodies. Eur. J. Biochem. 211, 99–104.

Aoubala, M., Bonicel, J., Benicourt, C., Verger, R., De Caro, A., 1994. Tryptic cleavage of gastric lipases. Location of the single disulfide bridge. Biochim. Biophys. Acta 1213, 319–324.

Aoubala, M., Ivanova, M., Douchet, I., De Caro, A., Verger, R., 1995. Interfacial binding of human gastric lipase to lipid monolayers, measured with an ELISA. Biochemistry 34, 10786–10793.

Arnett, E.M., Harvey, N.G., Rose, P.L., 1989. Stereochemistry and molecular recognition in two dimensions. Acc. Chem. Res. 22, 131–138.

Björkling, F., Dahl, A., Patkar, S., Zundel, M., 1994. Inhibition of lipases by phosphonates. Biorgan. Med. Chem. 2, 697–705.

Cygler, M., Grochulsi, P., Kazlauskas, R.J., Schrag, R.D., Bouthillier, F., Rubin, B., Serreqi, A.N., Gupta, A.K., 1994. A structural basis for the chiral preferences of lipases. J. Am. Chem. Soc. 116, 3180–3186.

De Caro, A., Figarella, C., Amic, J., Michel, R., Guy, O., 1977. Human pancreatic lipase: a glycoprotein. Biochim. Biophys. Acta 490, 411–419.

Drent, M.L., Vanderveen, E.A., 1993. Lipase inhibition: a novel concept in the treatment of obesity. Int. J. Obes. 17, 241–244.

Drent, M.L., Vanderveen, E.A., 1995. First clinical studies with orlistat: a short review. Obes. Res. 3, S623–S625.

Drent, M.L., Larsson, I., William-Olsson, T., Quaade, F., Czubayko, F., Vonbergmann, K., Strobel, W., Sjostrom, L., Vanderveen, E.A., 1995. Orlistat (Ro18-0647), a lipase inhibitor, in the treatment of human obesity: a multiple dose study. Int. J. Obes. 19, 221–226.

Egloff, M.-P., Marguet, F., Buono, G., Verger, R., Cambillau, C., van Tilbeurgh, H., 1995a. The 2.46 Å resolution struture of the pancreatic lipase-colipase complex inhibited by a C11 alkyl phosphonate. Biochemistry 34, 2751–2762.

Egloff, M.-P., Ransac, S., Marguet, F., Rogalska, E., van Tilbeurgh, H., Buono, G., Cambillau, C., Verger, R., 1995b. Les lipases: cinétiques, spécificités et aspects structuraux. Oléagineux, corps gras et lipides 2, 52–67.

Gargouri, Y., Piéroni, G., Ferrato, F., Verger, R., 1987. Human gastric lipase: a kinetic study with dicaprin monolayers. Eur. J. Biochem. 169, 125–129.

Gargouri, Y., Ransac, S., Verger, R., 1997. Covalent inhibition of digestive lipases. An in vitro study. Biochim. Biophys. Acta 1344, 6–37.

Güzelhan, C., Crijns, H.J.M.J., Peeters, P.A.M., Jonkman, J.H.G., Hartmann, D., 1991. Pharmacological activity (inhibition of fat absorption) and tolerability in healthy

volonteers of tetrahydrolipstatin (THL)—a specific lipase inhibitor. Int. J. Obes. 15 (suppl. 1), 29.

Güzelhan, C., Odink, J., Jansenzuidema, J.J.N., Hartmann, D., 1994. Influence of dietary composition on the inhibition of fat absorption by orlistat. J. Int. Med. Res. 22, 255–265.

Ivanova, M.G., Aoubala, M., De Caro, A., Daniel, C., Hirn, J., Verger, R., 1993. A study on human gastric lipase and complexes with monoclonal antibodies using the monomolecular film technique. Colloids Surf. B1, 17–22.

Maier, L., 1973. Organic phosphorus compounds 59. A new method for the synthesis of phosphonic dichlorides [1]. Hel. Chim. Acta 56, 492.

Mannesse, M.L.M., Boots, J.W.P., Dijkman, R., Slotboom, A.J., Vanderhijden, H.T.W.V., Egmond, M.R., Verheij, H.M., de Haas, G.H., 1995. Phosphonate analogues of triacylglycerols are potent inhibitors of lipases. Biochim. Biophys. Acta 1259, 56–64.

Marguet, F., Cudrey, C., Verger, R., Buono, G., 1994. Digestive lipases: inactivation by phosphonates. Biochem. Biophys. Acta 1210, 157–166.

Moreau, H., Abergel, C., Carrière, F., Ferrato, F., Fontecilla-Camps, J.C., Verger, R., 1992. Isoform purification of gastric lipases: towards crystallization. J. Mol. Biol. 225, 147–153.

Pathirana, S., Neely, W.C., Myers, L.J., Vodyanoy, V., 1992. Chiral recognition of odorant (+)- and (−)-carvone by phospholipids monolayers. J. Am. Chem. Soc. 114, 1404–1405.

Patkar, S., Björkling, F., 1994. Lipase inhibitors. In: Wooley, P., Petersen, S.B. (Eds.), Lipases. Their structure, biochemistry and application. Cambridge University Press, Cambridge, pp. 207–224 and references therein.

Perrin, D.D., Amarego, W.L.F., Perrin, D.R., 1980. Purification of laboratory chemicals, 2. Pergamon, Oxford.

Piéroni, G., Verger, R., 1979. Hydrolysis of mixed monomolecular films of triglyceride–lecithin by pancreatic lipase. J. Biol. Chem. 254, 10090–10094.

Piéroni, G., Verger, R., 1983. Hydrolysis of mixed monomolecular films of phosphatidylcholine–triacylglycerol by pancreatic phospholipase A2. Eur. J. Biochem. 132, 639–644.

Quast, H., Heuschmann, M., Abdel-Rahman, M.O., 1974. Preparation of methylphosphonic dichloride. Synthesis 490.

Ransac, S., Rivière, C., Soulié, J.M., Gancet, C., Verger, R., de Haas, G.H., 1990. Competitive inhibition of lipolytic enzymes. I. A kinetic model applicable to water-insoluble competitive inhibitors. Biochim. Biophys. Acta 1043, 57–66.

Ransac, S., Gargouri, Y., Moreau, H., Verger, R., 1991. Inactivation of pancreatic and gastric lipases by tetrahydrolipstatin and alkyl-dithio-5-(2-nitrobenzoic acid). A kinetic study with 1,2-didecanoyl-*sn*-glycerol monolayers. Eur. J. Biochem. 202, 395–400.

Ransac, S., Carriere, F., Rogalska, E., Verger, R., Marguet, F., Buono, G., Pinho Melo, E, Cabral, J.M.S., Egloff, M.-P., van Tilbeurgh, H., Cambillau, C., 1996. The specificities and structural features of lipases. In: Op den Kamp, J.A.F. (Ed.), NATO ASI Series H: Cell Biology, vol. 96. Springer, Berlin, pp. 265–304.

Rogalska, E., Nury, S., Douchet, I., Verger, R., 1995. Lipase stereo- and regio-selectivity towards three isomers of dicaprin, a kinetic study by the monomolecular film technique. Chirality 7, 505–515.

Rogalska, E., Nury, S., Douchet, I., Verger, R., 1997. Lipase stereo- and regio-selectivity towards tri- and di-glycerides. Biochem. Soc. Trans. 25, 161–164.

Rogalska, E., Ransac, S., Verger, R., 1990. Stereoselectivity of lipases. II. Stereoselective hydrolysis of triglycerides by gastric and pancreatic lipases. J. Biol. Chem. 265, 20271–20276.

Schmid, R.D., Verger, R., 1998. Lipases: interfacial enzymes with attractive applications. Angew. Chem. Int. Ed. 37, 1608–1633.

Stadler, P., Zandonella, G., Haalck, L., Spener, F., Hermetter, A., Paltauf, F., 1996. Inhibition of microbial lipases with stereoisomeric triradylglycerol analog phosphonates. Biochim. Biophys. Acta 1304, 229–244.

Still, W.C., Kahn, M., Mitra, A., 1978. Rapid chromatographic technique for preparative separation with moderate resolution. J. Org. Chem. 43, 2923–2925.

van Tilbeurgh, H., Egloff, M.-P., Martinez, C., Rugani, N., Verger, R., Cambillau, C., 1993. Interfacial activation of the lipase-procolipase complex by mixed micelles revealed by X-ray crystallography. Nature 362, 814–820.

Verger, R., de Haas, G.H., 1973. Enzyme reactions in a membrane model. 1: A new technique to study enzyme reactions in monolayers. Chem. Phys. Lipids 10, 127–136.

Vulfson, E.N., 1994. Industrial applications of lipases. In: Wooley, P., Petersen, S.B. (Eds.), Lipases. Their structure, biochemistry and application. Cambridge University Press, Cambridge, pp. 271–288.